공학박사 학위논문

Techno-economic Analysis and Energy Management System for Renewable Energy Micro-grid Under Climatic Variability

기후 변동성을 고려한 재생 에너지 기반 마이크로 그리드의 기술 경제성 분석 및 에너지 관리 기법 개발

2023년 2월

서울대학교 대학원
화학생물공학부
심 재 현

Techno-economic Analysis and Energy Management System for Renewable Energy Micro-grid Under Climatic Variability

지도교수 이 종 민

이 논문을 공학박사 학위논문으로 제출함

2023년 2월

서울대학교 대학원

화학생물공학부

심 재 현

심 재 현의 공학박사 학위논문을 인준함

2023년 2월

위 원 장 _____ (인)

부위원장 _____ (인)

위 원 _____ (인)

위 원 _____ (인)

위 원 _____ (인)

Abstract

Techno-economic Analysis and Energy Management System for Renewable Energy Micro-grid Under Climatic Variability

Jaehyun Shim
School of Chemical and Biological Engineering
The Graduate School
Seoul National University

Micro-grids based on renewable energy resources have become a pivotal technology to address the growth of global climate crisis. While renewable energy is essential for the micro-grids, it has an intermittent nature and strong uncertainty, thus the climatic variability is a key issue for the micro-grids. Nevertheless, previous micro-grid's techno-economic analyses have rarely taken account of climatic variability, and there have been few studies related to sizing and energy management of a multi-stack micro-grid. We exploit big data driven analysis and mixed-integer stochastic energy management to resolve these issues. Utilizing climate data from 13,488 regions in 218 countries, climatic variability in techno-economic analysis is investigated. After preprocessing the data via uniform manifold approximation and projection, the dimensionally reduced data are clustered using hierarchical density-based spatial clustering of applications with noise algorithm,

and optimal sizes of cluster's micro-grids are compared to each other clusters according to climate patterns. The effects of climate on the sizes and costs of micro-grids are revealed based on the climate sensitivity analyses, which emphasizes the need to take climatic fluctuations into account when designing micro-grids. To decide structures and sizes of stacks, we propose mixed-integer stochastic programming that is appropriate for energy management of a multi-stack micro-grid under climate uncertainty. Validation of the proposed method's performance is followed by verification of the climatic influences on design of a multi-stack micro-grid through each illustrative example. In conclusion, it is indicated that climatic variability takes a significant role in micro-grids based on renewable energy.

The contributions of this thesis can be written as follows: First, the correlation analysis through unsupervised clustering is carried out to verify that climatic variability is a factor that determine the design of techno-economical micro-grids. Mitigating their noise and clustering them via UMAP and HDBSCAN algorithm, climate data from 13,844 cities in 218 nations are used to the correlation analysis. Second, the strategies to install and operate a micro-grid during long project's lifespan are suggested according to regional climatic features. In third, a mixed-integer stochastic programming is developed to control a multi-stack micro-grid's energy distributions. Finally, it is verified that the climatic effects are noticeable in design of a multi-stack micro-grid.

Keywords: Micro-grid, renewable energy, big data analysis, techno-economic

analysis, sensitivity analysis, energy management system, mixed-integer stochastic programming, economies of scale

Student Number: 2017-22082

Contents

List of Tables

List of Figures

Chapter 1

Introduction

1.1 Motivation and previous work

Interest in the global climate crisis has growed since a global agreement to limit global warming to 2°C was reached by governments around the world at the Conference of the Parties in December 2015 [1]. The development of industrial technology raises the energy consumption rates, induces growth of CO_2 emissions, and pollutes the environment. Moreover, global temperatures have risen by 0.18 °C a decade according to the National Oceanic and Atmospheric Administration [2, 3]. To prevent the expansion of technology from accelerating the global climate crisis, pro-environmental power generation has been focused on and technologies related to power generation or power-to-gas using renewable energy sources have been investigated [4, 5]. A micro-grid utilizing renewable energy is suitable for eco-friendly electricity generation and hydrogen production, thus research on it has increased [6] In a micro-grid system, various combinations of equipment exist and it commonly comprises three types of equipment: electric generator, electrochemical converter, and storage units. Photovoltaic (PV) modules, wind turbines, and tidal generators are utilized as an electric gen-

erator, electrolyzers and fuel cells perform an main role as electrochemical reactors, and electrical energy and hydrogen are stored in batteries and hydrogen tanks, respectively.

To design an economic micro-grid, previous studies have implemented techno-economic analysis of a micro-grid using renewable energy. A micro-grid is categorized according to two criteria: hybrid energy sources or not, and stand-alone or not. While techno-economical micro-grids based solely on PV modules have been analyzed, hybrid micro-grids which consist of two types of electric generators such as PV modules and wind turbines have also been techno-economically optimized [7, 8, 9]. The problem regarding stand-alone micro-grid with hybrid renewable energies have been solved to find optimal sizes [10, 11, 12, 13, 14, 15]. Sizes in a stand-alone micro-grid have been investigated with rule-based operation in consideration of pollutant emission, life-cycle cost, and renewable energy penetration[16].

Given structure of a micro-grid, cost effective and secure operations necessitate energy management system (EMS) or control. Nonlinear programming, mixed-integer linear programming, dynamic programming, and model predictive control have been utilized to develop EMS for micro-grids [17]. In a smart wind power facility, two different methods, heuristic and linear programming method, were compared for EMS [7, 8, 9]. Genetic algorithm has been used to solve a pareto optimal problem that minimizes pollutant emission and total cost at the same time [18]. Due to intermittent nature of renewable energy and variability of load demands, uncertainty should be considered in EMS of a renewable micro-grid. A micro-grid has been operated using optimal explicit scheduling which is obtained on off-line in

advance via parametric programming [19]. SAM-theta-PSO algorithm has been suggested to manage energy distributions of a renewable micro-grid under consideration of uncertainty [20]. Two-stage stochastic programming has been suggested to consider sizes of a micro-grid and optimal operation strategy based on the scenarios [21].

In spite of assumption that each equipment exists as a single unit in most studies, multiple stacks of equipment are more realistic and have an advantageous of operating a micro-grid efficiently under intermittent nature of renewable energy. While the entire equipment should be operated regularly, a part of the equipment is enough to maintain system and meet load demands in a certain circumstance. A micro-grid composed of multiple stacks has an ability to cope with intermittency and achieves cost saving operations via scheduling on-off state of each stack. Researches on EMS of a multi-stack micro-grid have been investigated. Multi-stack fuel cells have been scheduled to operate equipment economically and meet load demands [22, 23, 24]. A multi-stack battery energy storage system comprising different types of batteries has been optimized to lengthen the battery lifetime [25]. For a multi-stack micro-grid, it is important to consider economies of scale since the smaller the size of the stack, the more expensive the stack [26]. Whereas a multi-stack micro-grid achieves cost efficient operations via more flexible on-off scheduling than micro-grid with single units, it is rather wasteful when stack's size becomes overly small (i.e., a trade-off between economies of scale and efficiency of operations). To maintain a micro-grid at a best operating level, climatic effects on operations should be considerate and it is reasonable to decide the number of stacks and their sizes based

on climate.

Management of energy distributions for a renewable micro-grid has been studied using robust or stochastic programming to consider climate uncertainty. Based on the robust optimization, the mixture composed of Nitrogen, liquid Petroleum gas, and hydrogen has been managed to maximize hydrogen injection under uncertainties of wind power [27]. Power generator and energy storage system have been scheduled their on-off states indicated as integer variables, and the cost function has been optimized using scenario based stochastic mix-integer linear programming [28, 29]. Suggesting constraints for state-of-charge in the battery as chance constraints, adaptively constrained model predictive control for a micro-grid has been developed [30].

Although previous studies have analyzed technical economies and managed energy distributions of micro-grids with various methods, there have been the lacks of research on design of a micro-grid correlated to climate variability. In particular, few researches on techno-economic analyses have been conducted in consideration of uncertainty and intermittent nature of climates [12, 13, 14, 15], whereas diverse approaches in energy management field have mainly focused on climatic variability and widely proposed robust or stochastic optimization methods [31, 32, 33, 27]. As global climate change becomes severe [34], the project for a micro-gird is inevitably affected by climate change due to its long-term lifespan, more than 20 years in usual, thus it is necessary to integrate climatic variability and the design of a micro-grid. Additionally, few studies have considered climatic effects on design of multi-stack micro-grids and investigated relationships between

economies of scale and efficiency of operations. To overcome these issues, we proposed novel approaches to analyze correlations climatic patterns to the design of a micro-grid and a trade-off between economies of scale and efficiency of operations under climatic variability.

1.2 Statement of contributions

The main objective of this thesis is to suggest design strategies of a techno-economic micro-grid in consideration of climate variability. Techno-economic analyses are investigated under 9 types of climatic patterns, and sensitivity of techno-economic micro-grids is analyzed for changing the climatic patterns. In addition, a mixed-integer stochastic programming for a multi-stack micro-grid is suggested to design it under climate variability. The performance of the suggested method is validated with an illustrative example, and two multi-stack micro-grids are designed to clarify climatic effects based on the proposed method. The summary of the two chapters are below:

- Global analysis of the impact of climatic patterns on economic designs of micro-grids through unsupervised clustering.
- Energy management and design of multi-stack micro-grid under climatic uncertainty using mixed-integer stochastic programming.

The first work is the techno-economnic analysis of micro-grid systems through unsupervised clustering. There is a direct correlation between the amount of renewable energy sources available in a region and the amount

of electricity generated, which relies on regional climatic characteristic. As a consequence, climatic patterns in the region influence techno-economic analysis of a micro-grid with renewable energy. We cluster climate-similar locations based on their climate data to separate climatic variability. Comparing techno-economic designs of micro-grids and climatic patterns, the correlations of them are evaluated, and it is determined which design would be advantageous in a particular climate pattern. Based on climate pattern changes, we also perform a sensitivity analysis of each group. The use of this information derived from big data is relevant to micro-grid design in actuality.

The second part is the mixed-integer stochastic programming for energy management and design of a multi-stakc micro-grid under climate variability. Suggested mixed-integer stochastic programming contains chance constraints for boundaries of state-of-charge in battery system, which handles stochastic effects of climate on a micro-grid. To take advantages of computational efficiency, chance constraints are converted to deterministic hard constraints with relaxation of joint chance constraints and assumptions that climate uncertainty is zero mean, independent, and identically distributed random variables. The overall method is applied to case study of scheduling a multi-stack micro-grid with real irradiance data in Washington, United States. Is is shown that the proposed method outperforms deterministic method. At last, the number of stacks and their sizes are decided via grid search based on the proposed method for two regions, and the importance of climatic effects on the design is verified.

1.3 Outline of the thesis

The remainder of the thesis is organized as follows. In Chapter **2**, the background on the algorithms for unsupervised clustering of climate data, and the model and cost equations of equipment in a micro-grid are introduced, and the overview of the stochastic model predictive control and stochastic tube method are provided. In Chapter **3**, micro-grids are optimized to conduct techno-economic analysis and correlations between optimal design and climatic patterns are discussed. In addition, sensitivity analysis of techno-economic designs is investigated with changing climatic patterns. Chapter **4** proposes a mixed-integer stochastic programming to manage energy distributions of a multi-stack micro-grid under climate uncertainty, and verifies effects of climatic patterns on a trade-off between economies of scale and efficient operations. Lastly, general concluding remarks and possible directions for further study are given in Chapter **5**.

Chapter 2

Background and preliminaries

2.1 Uniform manifold approximation and projection

Uniform manifold approximation and projection (UMAP) is widely used across the fields and is known for its nonlinear dimensionality reduction, which prevents features from overlapping and efficiently visualizes data. It has a lower computational cost than t-distributed stochastic neighborhood embedding (t-SNE), allowing it to extract features from very large or high-dimensional datasets [35, 36, 37]. UMAP constructs a high-dimensional data topology and discovers its low-dimensional representation by retaining topological linkages of the data [38]. Prior to reducing a dimension with UMAP, four parameters must be determined: the number of neighbors, minimum distance, number of components, and metric. When attempting to comprehend the complex structure of data, the number of neighbors represents the number of the local neighborhood. The fewer neighbors that are evaluated, the more localized components of the structure. Minimum distance is a numeric value between 0 and 1 indicating the minimum distance that low-dimensional points should be apart. The lower this value, the more dispersed the dots with low dimensions. Dimensionality of reduced

dimension space is determined by the number of components. Euclidean, Manhattan, and Chebyshev metrics are utilized to calculate the distances between points in high and low dimension space. Low dimensional representation varies based on these characteristics

2.2 Hierarchical density-based spatial clustering of applications with noise

Hierarchical density-based spatial clustering of applications with nois (HDBSCAN) is a density-based clustering approach that has been widely applied to climate and geographical data clustering [39, 40, 41]. Using mutual reachability distance to build a dendrogram for clustering, HDBSCAN method divides the data into several hierarchies. Then, clusters are identified by comparing each hierarchy based on a set of criteria, which is determined by the minimum cluster size and the minimum samples. Minimum cluster size refers to the smallest group deemed to be a cluster. Increasing the minimum cluster size increases the number of points contained in a cluster while decreasing the number of clusters. Minimum samples specifies the minimum number of neighbors around the cluster's center; the greater this value, the greater the number of points that are eliminated as noise.

2.3 Equipment's models used in micro-grid

Fig. 3.1 shows a diagram of a micro-grid to be dealt with in this study. To simulate each unit, a simple linear model was employed as opposed to a sophisticated nonlinear dynamic model. Researches for techno-economic

analysis of micro-grid have implemented size optimization based on a simple linear model or Hybrid Optimization of Multiple Energy Resources (HOMER) Pro which also uses a simple linear model [11, 42, 14]. In this work, computational efficiency is crucial because the total number of optimization problems to be solve is 55,376, which was accomplished through the use of linear models. The optimization problem was formulated using mixed-integer linear programming (MILP), where the unit sizes are the design variables [10, 11, 42] and Table 3.2 lists the parameters for the model equations.

2.3.1 PV module

We assume one PV module exists in the P2G network, where the power is generated by sunlight. The hourly power output of the PV module depends on solar irradiance and temperature as follows [10]:

$$P_{PV}(t) = \frac{G(t)}{G_{STC}} P_{PV}^{rat} \eta_{PV} \left[1 - \beta \left(T_C - T_{C,STC}\right)\right] \tag{2.1}$$

where P_{PV} is the output power from the PV module, $G(t)$ is the solar irradiance, G_{STC} is the solar irradiance under standard test conditions (STC), PV_{PV}^{rat} is the rated power of the PV module, η_{PV} is the power reduction factor, β is the temperature coefficient of the PV module, T_C is the PV cell temperature, and $T_{C,STC}$ is the PV cell temperature under STC.

2.3.2 Wind turbine

The power generated from the wind turbine is given as a conditional function of the wind speed as follows [11]:

$$P_{WT}(t) = \begin{cases} 0, & \text{if } v \leq v_{cut-in} \text{ or } v > v_{cut-out} \\ P_{WT}^{rat}\left(\frac{v^3 - v_{cut-in}^3}{v_r^3 - v_{cut-in}^3}\right), & \text{if } v_{cut-in} < v \leq v_r \\ P_{WT}^{rat}, & \text{if } v_r < v \leq v_{cut-out} \end{cases} \tag{2.2}$$

where P_{WT} is the output power from the wind turbine and P_{WT}^{rat} is the rated power of the wind turbine at its rated wind speed. v, v_r, v_{cut-in}, and $v_{cut-out}$ represent the current wind speed, rated speed, cut-in speed, and cut-out speed, respectively.

The first conditional equation represents situations in which the operation is halted due to insufficient wind speed or to prevent damage from operating outside of the permissible range.

2.3.3 Electrolyzer

The water electrolyzer, which splits water into hydrogen and oxygen, is a viable and commonly employed process unit for hydrogen production. In commercial markets, an alkaline or proton-exchange membrane electrolyzer is often preferred. In a simple linear model, the electrolyzer's hydrogen generation rate is proportional to the input power, and its conversion equation is [12]:

$$P_{EZ} = \frac{\dot{m}_{H_2} HHV_{H_2}}{\eta_{EZ}} \tag{2.3}$$

where P_{EZ} is the input power consumed in the electrolyzer, $\dot{m}_{H_2}$ is the electrolyzer's hydrogen production mass flow rate, HHV_{H_2} is the higher heating value of hydrogen, and η_{EZ} is the electrolyzer efficiency.

2.3.4 Fuel cell

A fuel cell converts hydrogen into electricity, and due to its physical simplicity, solid oxide fuel cells (SOFC) are commonly preferred for P2G systems. The generated power of SOFC is proportional to the amount of hydrogen used as follows [42]:

$$\eta_{FC} = \frac{P_{FC}}{\dot{m}_{H_2} HHV_{H_2}} \tag{2.4}$$

where P_{FC} is the output power produced by the fuel cell, $\dot{m}_{H_2}$ is the hydrogen production mass flow rate entering the fuel cell, and η_{FC} is the fuel cell efficiency.

2.3.5 Energy storage - battery and hydrogen tank

The electric power generated in the micro-grid can be stored in batteries or tanks, as either electricity or hydrogen. The simplest battery model considers only charge and discharge rate and expresses state-of-charge (SoC) as the quantity of power charged within the battery. The SoC is a function

of the input current as follows [42]:

$$SoC(t) = SoC(0) + \frac{1}{C}\int_0^t \left(\eta_{char} I_{char} - \eta_{dis} I_{dis}\right)(t')dt' \tag{2.5}$$

where C represents the capacity for batteries, I_{char} represents the charge current, and I_{dis} represents the discharge current. η_{char} and η_{dis} represent the charge and discharge efficiencies of a battery in relation to energy loss.

To simulate the amount of hydrogen stored in a tank, a simple model that defines state-of-hydrogen (SoH) as an expression for ratio stored hydrogen to a tank capacity is used [12]:

$$SoH(t) = SoH(0) + \frac{1}{C_{H_2}}\int_0^t \left(\eta_{sto}\dot{H}_{2sto} - \eta_{rel}\dot{H}_{2rel}\right)(t')dt' \tag{2.6}$$

where C_{H_2} is the capacity of the hydrogen tank, $\dot{H}_{2sto}$ is the flow rate of stored hydrogen, and $\dot{H}_{2rel}$ is flow rate of released hydrogen. The store and release efficiencies for hydrogen tank are denoted by η_{sto} and η_{rel}, respectively.

2.4 Net present cost

The objective of micro-grid design is to minimize the overall cost of installation, operation, and maintenance for a particular climate (i.e., irradiance and wind speed) and energy source requirements (i.e., hydrogen and electricity).

Net present cost (NPC) is the most widely used metric for techno-economic assessment of micro-grid. HOMER Pro optimizes P2G process by minimizing NPC [43] and is commonly used in the field to analyze micro-grid architecture [44, 45]. NPC includes costs and salvages incurred over the lifetime of the project [12, 13].

Assuming that each unit is depreciated linearly and salvage value is dependent on replacement cost, the NPC of a micro-grid is calculated as:

$$\begin{aligned} NPC &= C_{cap} + \sum_{n=1}^{N} i_d \cdot C_{OM} + i_d^N \left(C_{rep} Integer \left(\frac{N}{Rep} \right) - S \right) \\ S &= C_{rep} \frac{Rem}{Rep} \\ i_d &= \frac{1}{(1+i_r)^n} \\ i_d^N &= \frac{1}{(1+i_r)^N} \\ i_r &= \frac{i_n - f}{1+f} \end{aligned} \tag{2.7}$$

where N is the project lifetime in years, C_{cap} is the capital cost of a unit, C_{OM} is the operation and maintenance (O&M) cost of a unit, C_{rep} is the replacement cost of a unit, S is the salvage value of a unit, Rep is the lifetime of a unit, Rem is the remaining lifetime at the end of the project, i_d is the discount rate, i_r is the annual real interest rate, i_n is the nominal interest rate, and f is the annual inflation rate. Depending on geological area and operational conditions, the costs and lifetime of process units vary. These values were determined in our study using the same specifications as in prior studies [12, 13, 46] (Table 2.1).

Table 2.1: Specifications of micro-grid

	Capital cost	O&M cost	Replacement cost	lifetime
PV module	3000 \$/kW	10 \$/kW/year	3000 \$/kW	25 years
Wind turbine	2000 \$/kW	20 \$/kW/year	2000 \$/kW	20 years
Electrolyzer	2000 \$/kW	10 \$/kW/year	2000 \$/kW	15 years
Fuel cell	3000 \$/kW	10 \$/kW/year	3000 \$/kW	4.5 years
Battery	450 \$/kWh	5 \$/kWh/year	450 \$/kWh	15 years
Hydrogen tank	1500 \$/H_2 kg	10 \$/H_2 kg/year	1500 \$/H_2 kg	25 years

2.5 Stochastic model predictive control

Stochastic model predictive control (SMPC) is an MPC methodology that includes a model, objective function, and constraints with stochasticity. The optimization problem of SMPC is shown in Equation 2.8a. Equation 2.8a represents the expected value of the quadratic objective function for a given disturbance realization. Equation 2.8a represents the linear time-invariant model with additive disturbance. Equation 2.8a indicates the constraints of the optimization problem. The constraints applied to the state $x_{k+i+1|k}$ are chance constraints that limit the probability of a violation. The probability of violation can be tuned by adjusting the risk parameter β. The stochastic components of SMPC optimization problem should be reformulated into a form usable by conventional optimization solvers.

$$\min_{U} E\left[\sum_{i=0}^{N-1}\left(x_{k+i|k}^{T} Q x_{k+i|k} + u_{k+i|k}^{T} R u_{k+i|k}\right) + x_{k+N}^{T} P x_{k+N}\right] \tag{2.8a}$$

$$\textit{s.t.} \quad x_{k+i+1|k} = A x_{k+i|k} + B u_{k+i|k} + D w_{k+i|k} \tag{2.8b}$$

$$Pr\left[H x_{k+i+1|k} \leq h\right] \geq \beta, \quad u_{k+i|k} \in U, \quad x_{k|k} = x(k) \tag{2.8c}$$

$$\forall i \in 0, ..., N-1 \tag{2.8d}$$

2.5.1 Stochastic tube model predictive control

The SMPC can be formulated as a stochastic tube MPC to approximate the stochastic model, objective function, and chance constraint into deterministic form. The optimization problem of stochastic tube MPC is shown in Equation 2.5.1. Stochastic tube MPC separates the stochastic term by dividing the state $x_{k+i+1|k}$ into a deterministic term $z_{k+i+1|k}$ and a zero-mean disturbance term $e_{k+i+1|k}$. Also, it separates the stochastic term by dividing the input $u_{k+i+1|k}$ into a static feedback term $-Kx_{k+i|k}$ and input $v_{k+i+1|k}$. Equation 2.9a represents the reformulated quadratic objective function. The expectation term disappears by the assumption that $e_{k+i|k}$ has a zero-mean distribution. Equation 2.9b represents deterministic model and Equation 2.9d represents disturbance propagation, where K is LQR gain. Equation 2.9e represents the reformulated chance constraints using $F_{k+i+1|k}$, the cumulative density function of $Hz_{k+i+1|k} - h$.

$$\min_{U} \sum_{i=0}^{N-1} \{z_{k+i|k}^T Q z_{k+i|k} + v_{k+i|k}^T R v_{k+i|k}\} + z_{k+N}^T P z_{k+N} \tag{2.9a}$$

$$\textit{s.t.} \quad z_{k+i+1|k} = Az_{k+i|k} + Bv_{k+i|k} \tag{2.9b}$$

$$u_{k+i|k} = -Kz_{k+i|k} + v_{k+i|k} \tag{2.9c}$$

$$e_{k+i+1|k} = (A - BK)e_{k+i|k} + Dw_{k+i} \tag{2.9d}$$

$$Hz_{k+i+1|k} \leq F^{-1}_{k+i+1|k}(1-\beta) \tag{2.9e}$$

$$u_{k+i+1|k} \in U, \quad z_{k|k} = x(k), \quad e_{k|k} = 0 \tag{2.9f}$$

$$\forall i \in 0, ..., N-1 \tag{2.9g}$$

Chapter 3

Techno-economic analysis of micro-grid system design through climate region clustering [1]

3.1 Introduction

The expansion of industrial technology raises the rate of energy consumption and CO_2 emissions. Consequently, interest in the global climate crisis is growing, and in December 2015, at the Conference of the Parties, governments from around the world resolved to limit global temperature rise to 2°C [1]. According to the NOAA (National Oceanic and Atmospheric Administration), 2019 was the second warmest year on record, and the world annual average temperature has risen at a rate of 0.18 °C each decade, which is twice as fast as before 1981 [2, 3]. Hydrogen has emerged as a green fuel, and research on eco-friendly power generation utilizing renewable energy has increased [4, 5]. To produce hydrogen without polluting the environment, the micro-grid utilizing renewable energy has been investigated [6]. For micro-grid system, there are three types of process units: electric generator, electrochemical converter, and storage units. Common

[1] This chapter is an adapted version of J. H. Shim, D. D. Park, H. T. Chung, H. C. Ryu, G. B. Choi, and J. M. Lee, "Techno-economic analysis of micro-grid system design through climate region clustering," *Energy Conversion and Management*, 274, 116411.

electric generators include photovoltaic (PV) modules, wind turbines, and tidal generators. Electrolyzers and fuel cells are the main electrochemical reactors of micro-grid systems. The electrolyzer converts electricity into hydrogen through the electrolysis of water, whereas the fuel cell produces power from hydrogen through the inverse reaction. Batteries and hydrogen tanks are used to store electrical energy and hydrogen, respectively. Previous studies have investigated the optimal sizes for these units. Hybrid micro-grids comprising PV module, wind turbine, diesel generator, electrolyzer, fuel cell, and a load have been optimized [7, 8, 9]. The problem of sizing a stand-alone micro-grid with hybrid renewable energy sources has been solved [10, 11, 12, 13, 14, 15]. There have been also studies on managing energy distributions for the efficient and secure operation of a micro-grid. A comparison was made between heuristic and linear programming methods for energy management in a smart wind power facility [7, 8, 9]. A pareto optimal problem has been solved using a genetic algorithm in order to find an optimal scheduling that minimizes total cost and pollutant emission simultaneously [18]. Considering sizes of a micro-grid and optimal operation strategy, two-stage stochastic programming based on the scenario has been calculated [21]. Energy management systems have been developed via various methods such as nonlinear programming, mixed-integer linear programming, dynamic programming, and model predictive control [17].

Climates have strong uncertainty and intermittent nature, hence climatic variability should not be overlooked in renewable energy research. While energy management problems have widely adopted robust or stochastic optimization methods to handle the variability [31, 32, 33, 27], the vast

majority of techno-economic analyses were conducted based solely on a single year's worth of weather data, such as irradiance and wind speed data for a specific region, thereby ignoring climatic variability [12, 13, 14, 15]. Incorporating climatic variability into the design of a micro-grid system becomes crucial as the severity of climate change increases [34]. Given that the average project lifespan is greater than 20 years, climate change is inevitable during the project's lifetime and it is crucial to build for it from the outset Only when sufficiently different data are available can climatic variability be characterized, which is often not the case when focusing on data from a single region.

To overcome these issues, we offer a novel approach that clusters climate-similar locations and integrates their climate data to evaluate climatic variability. Global climate data were gathered from the Prediction of Worldwide Energy Resource (POWER) Project's Hourly 2.0.0 version on 2022/01/21. [47]. The collection includes hourly data for 13,844 regions in 218 countries for a period of one year. The optimal sizing is then conducted for each cluster and its dependence on climate patterns is analyzed. As opposed to examining each region individually, 13,844 regions were clustered into different groups based on climate patterns and their relationships with optimization results were evaluated . Clustering and analysis consist of two steps. We use uniform manifold approximation and projection (UMAP) [38] to extract two characteristic features from high-dimensional climate data, followed by the hierarchical density-based spatial clustering of applications with noise (HDBSCAN) algorithm [48, 49]. We determine the climatic features and which regions are included based on the clustering . Comparing the geo-

graphical location, climate characteristics and optimal sizes, the climatic factors affecting the optimal design were derived and the design that would be advantageous in a given climate pattern was identified. A climate sensitivity analysis of the optimal design has also been conducted. Instead of conducting an analysis with pointless and tiresome tweaks, we recognized a pattern in climate change of each group and conducted a sensitivity analysis that reflected it. Through this approach, we confirmed the patterns of sizing process units based on climate, identified areas vulnerable to climate change, and proposed new strategies for climatic variability. This information derived from big data is pertinent to the actual design of P2G systems when project lifespan is considered.

In Sections 2.3 and 3.2.3, modeling and optimization for micro-grid systems were formulated. Section 3.1 offers information on how to execute dimensionality reduction and clustering of the data and climate patterns for each group. Comparing the optimal sizes of each cluster to the climate, we uncover their relationships in Section 3.2. In Section 3.3, we figure out the effects of regional climatic variability on optimal sizes and analyze the climate change sensitivity of each cluster.

3.2 Methods

3.2.1 Climatic feature extraction by UMAP

For design of hybrid micro-grids with PV module and wind turbine, we collected irradiance and wind speed data for 8,760 hours by scraping open sources in National Aeronautics and Space Administration (NASA) Lang-

ley Research Center and implemented clustering based on the data. 13,844 regions in 218 countries were covered, and the country names are described in the Appendix. While 8,760 hours data were used for the optimization problem, they are too noisy to be used for clustering without preprocessing. In order to reduce the effect of noise, 8,760 hours data were smoothed and turned into 365 days of data for irradiance and wind speed with each data point derived from the daily average of 24 hours of data. Given two distinct types of data, the feature vector has a dimension of 730. In order to reduce the computational cost of clustering and visualization, the core features of the data was first extracted via UMAP. By lowering the dimension of the data in the clustering the curse of dimensionality is also avoided.

UMAP is widely used across the fields and is known for its nonlinear dimensionality reduction, which prevents features from overlapping and efficiently visualizes data. It has a lower computational cost than t-distributed stochastic neighborhood embedding (t-SNE), allowing it to extract features from very large or high-dimensional datasets [35, 36, 37]. UMAP constructs a high-dimensional data topology and discovers its low-dimensional representation by retaining topological linkages of the data [38]. Prior to reducing a dimension with UMAP, four parameters must be determined: the number of neighbors, minimum distance, number of components, and metric. When attempting to comprehend the complex structure of data, the number of neighbors represents the number of the local neighborhood. The fewer neighbors that are evaluated, the more localized components of the structure. Minimum distance is a numeric value between 0 and 1 indicating the minimum distance that low-dimensional points should be apart. The lower this

value, the more dispersed the dots with low dimensions. Dimensionality of reduced dimension space is determined by the number of components. Euclidean, Manhattan, and Chebyshev metrics are utilized to calculate the distances between points in high and low dimension space. Low dimensional representation varies based on these characteristics; hence, a grid search was conducted to obtain a low-dimensional structure that accurately depicts the relationship between data, with the exception of the number of components, which was fixed at 2. Table 3.1 displays the change range and interval for the parameters.

3.2.2 Clustering climate groups by HDBSCAN

To cluster and handle a characteristics of climatic data, density-based clustering algorithm has been used in the previous studies [50, 51, 52, 53]. HDBSCAN is a density-based clustering approach that has been widely applied to climate and geographical data clustering [39, 40, 41]. Using mutual reachability distance to build a dendrogram for clustering, HDBSCAN method divides the data into several hierarchies. Then, clusters are identified by comparing each hierarchy based on a set of criteria, which is determined by the minimum cluster size and the minimum samples. Minimum cluster size refers to the smallest group deemed to be a cluster. Increasing the minimum cluster size increases the number of points contained in a cluster while decreasing the number of clusters. Minimum samples specifies the minimum number of neighbors around the cluster's center; the greater this value, the greater the number of points that are eliminated as noise. Due to the fact that the validity of clustering also differs based on two param-

eters, grid search was utilized to cluster the climate data characteristics so that they are correctly separated. Table 3.1 displays the change range and interval for the parameters.

Density Based Clustering Validation (DBCV) is suited for density-based clustering algorithms since it captures the shape attribute of clusters via densities rather than distances. A weighted sum of cluster validity index values ranging from -1 to 1 is calculated [54]. Close to 1 implies a superior clustering result, and DBCV is used to evaluate grid search outcomes.

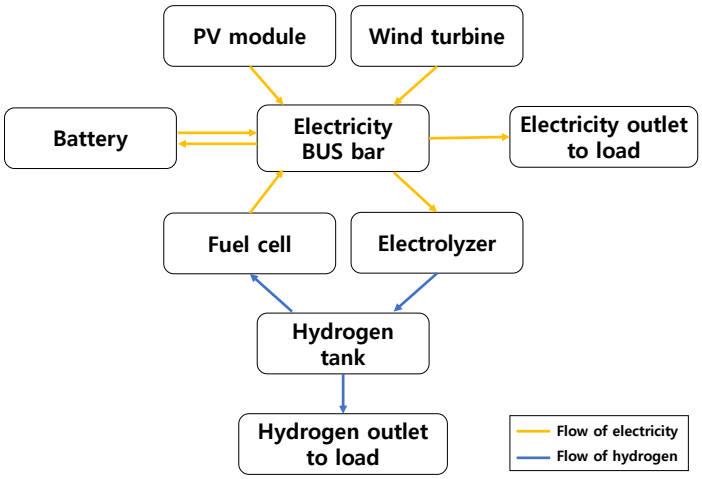

Figure 3.1: Diagram of a micro-grid.

Table 3.1: Parameter tuning for UMAP and HDBSCAN

	Parameter	Min	Max	Interval	Selected parameter
HDBSCAN	Minimum cluster size	100	1000	100	400
	Minimum samples	100	1000	100	100
UMAP	Number of neighbors	100	1000	100	800
	Minimum distance	0.0	0.9	0.1	0.0
	Metric	euclidean, manhattan, chebyshev			euclidean

Table 3.2: Parameters for models in a micro-grid

Parameter	Value
G_{STC}	1000 W/m^2
T_C	25 °C
$T_{C,STC}$	25 °C
v_r	20 m/s
v_{cut-in}	2.8 m/s
$v_{cut-out}$	25 m/s
HHV_{H_2}	39.4 kWh/kg
η_{EZ}	0.7
η_{FC}	0.55
η_{char}	0.95
η_{dis}	0.95
η_{sto}	0.95
η_{rel}	0.95
SoC_{min}	0.1
SoC_{max}	0.9
SoH_{min}	0
SoH_{max}	0.95

3.2.3 Problem formulation

The objective of micro-grid design is to minimize the overall cost of installation, operation, and maintenance for a particular climate (i.e., irradiance and wind speed) and energy source requirements (i.e., hydrogen and electricity). The design variables are the unit sizes of the micro-grid. The unit sizes of the micro-grid are optimized using the model equation of each unit above (Equations 2.1- 2.6), the objective function and constraints to be describe following.

3.2.3.1 Objective function

Since the optimization problem is implemented with a one-year time horizon as opposed to the entire project's lifetime, the cost of the each unit must be annualized for a fair comparison between components with varied capital and operating costs [43]. The annualized cost (AC) of a component can be calculated with the capital recovery factor (CRF) as follows [14]:

$$\begin{aligned} AC &= NPC \cdot CRF \\ CRF &= \frac{i\left(1+i_r\right)^N}{\left(1+i_r\right)^N - 1} \end{aligned} \tag{3.1}$$

Note that above costs are defined as the cost per unit size, therefore, the objective function J is the sum of the size of each unit multiplied by AC.

$$J = P_{PV}^{rat} AC_{PV} + P_{WT}^{rat} AC_{WT} + P_{EZ}^{rat} AC_{EZ} + P_{FC}^{rat} AC_{FC} + C \cdot AC_{Ba} + C_{H_2} \cdot AC_{HT} \tag{3.2}$$

where AC_{PV}, AC_{WT}, AC_{EZ}, AC_{FC}, AC_{Ba}, and AC_{HT} are the annualized cost of PV module, wind turbine, electrolyzer, fuel cell, battery, and hydrogen tank respectively. The sizes of each unit, P_{PV}^{rat}, P_{WT}^{rat}, P_{EZ}^{rat}, P_{FC}^{rat}, C, and C_{H_2}, are variables for optimization and determined to minimize the cost while satisfying the constraint conditions.

3.2.3.2 Constraints

There are several constraints to design a realistic micro-grid. First, the physical limitations of each process unit should be considered as follows [10, 46]:

$$\begin{aligned} SoC_{min} \leq SoC(t) \leq SoC_{max} \\ SoH_{min} \leq SoH(t) \leq SoH_{max} \\ P_{EZ}^{min} \leq P_{EZ}(t) \leq P_{EZ}^{max} \\ P_{FC}^{min} \leq P_{FC}(t) \leq P_{FC}^{max} \end{aligned} \tag{3.3}$$

where SoC_{min} and SoC_{max} are maximum and minimum SoC for battery, SoH_{min} and SoH_{max} are maximum and minimum SoH for hydrogen tank, P_{EZ}^{min} and P_{EZ}^{max} are maximum and minimum consumed power for electrolyzer, and P_{FC}^{min} and P_{FC}^{max} are maximum and minimum produced

power for fuel cell. P_{EZ}^{min} and P_{FC}^{min} are set to zero indicating that the device is powered off. P_{EZ}^{min} and P_{FC}^{min} are set to P_{EZ}^{rat} and P_{FC}^{rat} respectively as a definition of rated power.

One of the objective of micro-grid design is to meet energy requirements, and is achieved as constraints instead of including it in the objective function.

$$\begin{aligned} \|EL(t) - EL^{SP}(t)\| &\leq \epsilon \\ \|HL(t) - HL^{SP}(t)\| &\leq \epsilon \\ EL(t) = -P_{EZ}(t) + P_{FC}(t) - C\left(\eta_{char} I_{char} - \eta_{dis} I_{dis}\right) & \\ + P_{PV}(t) + P_{WT}(t) & \\ HL(t) = \dot{m}_{H_2}^{EZ} - \dot{m}_{H_2}^{FC} - C_{H_2}\left(\eta_{sto}\dot{m}_{H_2,sto} - \eta_{rel}\dot{m}_{H_2,rel}\right) & \end{aligned} \tag{3.4}$$

where $EL(t)$ and $EL^{SP}(t)$ are a electricity production rate to load demand and its set point, $HL(t)$ and $HL^{SP}(t)$ are a hydrogen production rate to load demand and its set point, and ϵ is a threshold for load demands with a small value.

Using the Big M approach, a conditional function of a wind turbine is expressed as a linear combination of two binary variables to generate a mixed-integer linear program.

$$
\begin{aligned}
P_{WT}(t) &= z_1 P_{WT}^{rat} \left(\frac{v^3 - v_{cut-in}^3}{v_r^3 - v_{cut-in}^3} \right) + z_2 P_{WT}^{rat} \\
(z_1 - 1)\, M &\leq (v - v_{cut-in} + \epsilon)\,(v_r - v + \epsilon) \leq z_1 M \\
(z_2 - 1)\, M &\leq (v - v_r - \epsilon)\,(v_{cut-out} - v + \epsilon) \leq z_2 M
\end{aligned}
\tag{3.5}
$$

where M is a very large positive value for Big M method and z_1 and z_2 are two binary variables. If v is between v_{cut-in} and v_r, then z_1 is 1, z_2 is 0, and $P_{WT}(t)$ equals to $P_{WT}^{rat} \left(\frac{v^3 - v_{cut-in}^3}{v_r^3 - v_{cut-in}^3} \right)$. If v is between v_r and $v_{cut-out}$, then z_1 is 0, z_2 is 1, and $P_{WT}(t)$ equals to P_{WT}^{rat}. If v is below v_{cut-in} or above $v_{cut-out}$, z_1, z_2, and $P_{WT}(t)$ becomes 0.

3.2.3.3 Load demands

Electricity and hydrogen load requirements were taken into account. In general, their values are described as random variables whose patterns include a decrease at night and an increase during the day, as well as seasonal and geographic variation in demand [55, 56, 57]. To examine the climate effect, we assumed that the demand for energy and hydrogen is the same in all places and only considered a specific pattern within 24 hours, ignoring seasonal and regional patterns. The load requirements were arbitrarily generated by adding white noise to a sine function. The range of the electricity load demand was between 0.5 and 5 kW/hr and the range of the hydrogen load demand was between 1 and 2 kg/hr.

3.3 Result and discussion

3.3.1 Feature extraction and clustering of regional climate

Before clustering via HDBSCAN, to verify that HDBSCAN is proper to cluster and manage climatic data according to their characteristics, clustering results using various clustering algorithms were compared to each other. Clustering algorithms are largely divided into partitional clustering, hierarchical clustering, and density-based clustering, and representative algorithms were selected for each type clustering respectively: K-means clustering as a partitional clustering, Agglomerative clustering as a hierarchical clustering, and the OPTICS algorithm as a density-based clustering. Grid searches were performed for entire algorithms while changing the parameters of UMAP and each algorithm. Silhoutte coefficients were used to assess the cluster's separability. According to [58], the Silhoutte coefficient represents the relative distance between points classified as belonging to the same cluster and points classified as belonging to a different cluster. A value close to 1 indicates that the cluster is distant from other clusters, while a value close to -1 indicates the clusters are intermingled. To cluster feature data using the algorithms, parameters should be determined in advance: the number of clusters should be determined for K-means clustering and Agglomerative clustering, and the minimum samples and metric for OPTICS algorithm. For each clustering method, grid search was implemented while changing the parameters, and the parameter with the highest Silhoutte coefficient was selected. K-means clustering separated features into 7 groups and its Sil-

houtte coefficient is 0.63, Agglomerative clustering divided features into 5 groups and its Silhoutte coefficient is 0.62, and OPTICS algorithm clustered features into 7 groups and its Silhoutte coefficient is 0.42. According to the Silhouette coefficient, K-means clustering and Agglomerative clustering seemed to separate features reliably whereas OPTICS algorithm was failed. However, K-means clustering and Agglomerative clustering also show limitations in separation. As shown in Fig. 3.2, two algorithms separated same feature data, i.e., their clustering results are based on the same UMAP parameters. Agglomerative clustering did not classify the climates enough to characterize their patterns, and in particular, it seems reasonable to separate group 1 of the Agglomerative clustering into two groups: group 2 and group 5 of the K-means clustering. For K-means clustering, the boundary dividing Group 3 and 7 doesn't seem reasonable since there is a lack of basis for separating the data near the boundary by a line, which is the limitation of partitional clustering. Therefore, the algorthms identified above are inadequate for clustering climate data, and more complex method need to be applied: the HDBSCAN was used in this study.

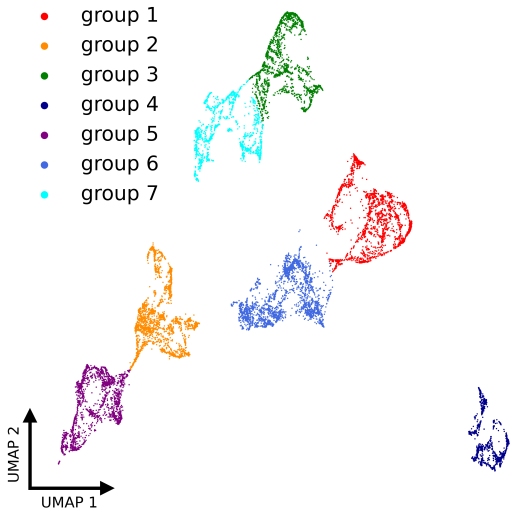

(a)

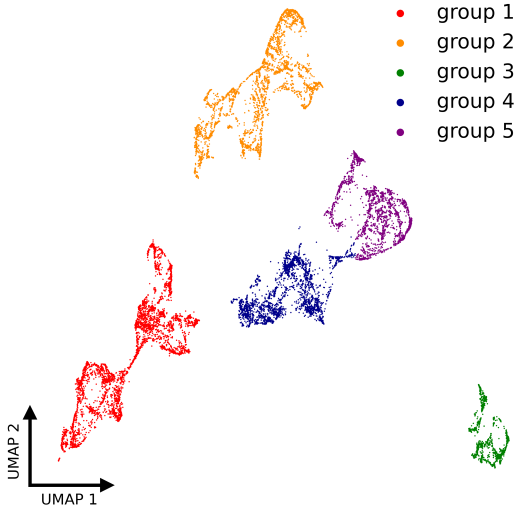

(b)

Figure 3.2: Feature maps of regional climate data, (a) clusterd features using K-means clustering, (b) clusterd features using Agglomerative clustering.

As shown in Table 3.1, we searched 30,000 cases using a grid search and initially excluded results divided into fewer than five, as climates in the world would be heuristically divided into at least five regions: near the equator, mid north latitude, high north latitude, mid south latitude, and high south latitude. Then, cases with a DBCV score below 0.5 were eliminated. The final instance was selected heuristically from the remaining cases based on the climate graph of each cluster. Table 3.1 shows the selected case parameters for UMAP and HDBSCAN. The cluster separability is reliable given that the validation value of the clustering result was 0.61. Figs.3.3a and 3.3b show the results of applying UMAP and HDBSCAN with the selected parameters. Each point in Fig. 3.3a represents a region and its position coordinate value is a 2-dimensional feature of irradiance and wind speed in the region. When points are close together and in the same cluster, they have comparable climates, and when they are far apart and in a separate cluster, they have diverse climates. The regions are clustered into nine groups and climate and regional characteristics for each group were evaluated.

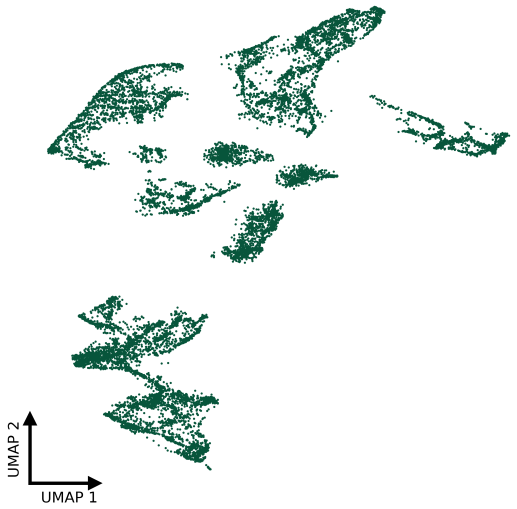

(a)

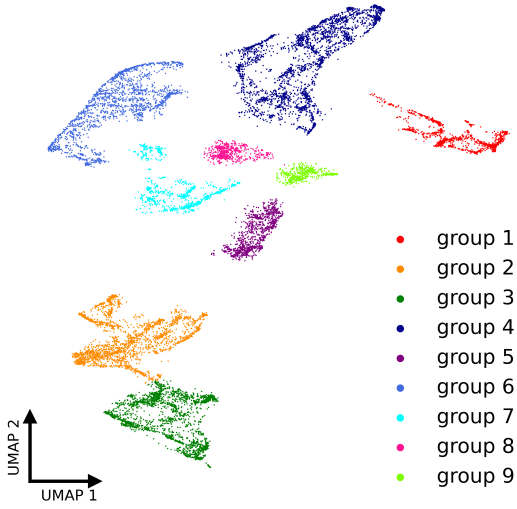

(b)

Figure 3.3: Feature maps of regional climate data, (a) two-dimensional extracted features using UMAP, (b) clusterd features using HDBSCAN.

Table 3.3: Top 3 countries in each group and the number of regions in each country.

Group	Country	Number of regions
1	China	809
	Japan	189
	South Korea	45
2	India	628
	Mexico	256
	Indonesia	144
3	Brazil	844
	Australia	497
	Argentina	265
4	France	376
	United States	364
	Russia	352
5	United States	464
	Iran	146
	Turkey	88
6	United States	1526
	Canada	278
	Japan	23
7	United States	853
	China	54
	Mexico	27
8	Spain	230
	Italy	133
	Portugal	61
9	Italy	109
	France	45
	Bulgaria	37

Table 3.3 shows the top three nations in each group, as well as the number of regions in each nation. As a result of climate similarity, neighboring countries are grouped together; for example, the United States and Canada are in Group 6. If the latitudes are comparable, locations on different continents are classified into the same group, for instance, India and Mexico are both in Group 2. Some nations such as the United States are included in multiple groups, indicating that their climates are diverse. The clustered features indicate geolocational climate characteristics such as annual mean values and graph shape (see Fig. 3.4 and 3.5). Group 1 consists of locations in China, Japan, and South Korea, all of which have a rainy season. The rainy season around June generates a plateau-like pattern in the annual irradiance. In Group 2, India, Mexico, and Indonesia are located close to the equator. Group 2 has a relatively high and consistent yearly irradiance, which is characteristic of climate patterns around the equator. Group 3 comprises the majority of regions in the Southern Hemisphere (e.g., Brazil, Australia, and Argentina), and has a typical pattern of irradiance that is low around June and high at the end and beginning of the year. Group 5 has a typical Northern Hemisphere irradiance pattern, which is shared by the subsequent groups. They are classified by annual average or annual difference of irradiance and wind speed patterns. The Group 4 and Group 6 regions have an annual wind speed of over 6 m/s and low irradiance; their geographic locations include Russia and Canada at high northern latitudes. Despite having comparable magnitudes and patterns of wind velocity, their annual average irradiance differs significantly, classifying the regions into two distinct groups (see Fig. 3.5 and Table 3.4).

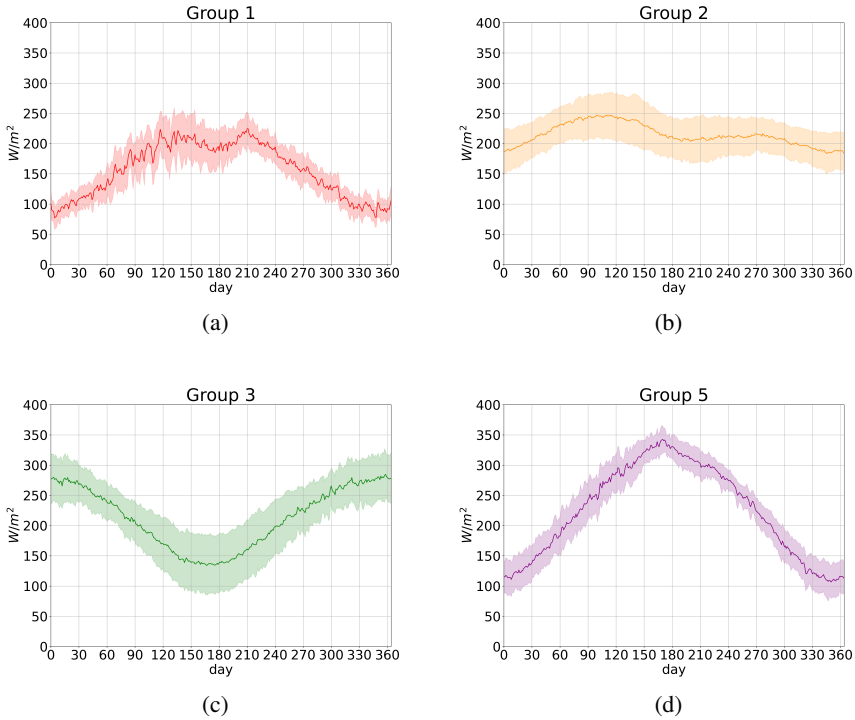

Figure 3.4: Irradince in a year of each group, (a) Group 1, (b) Group 2, (b) Group 3, (b) Group 5.

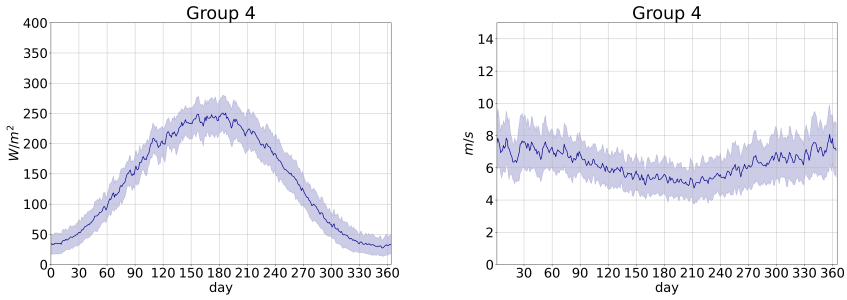

(a)

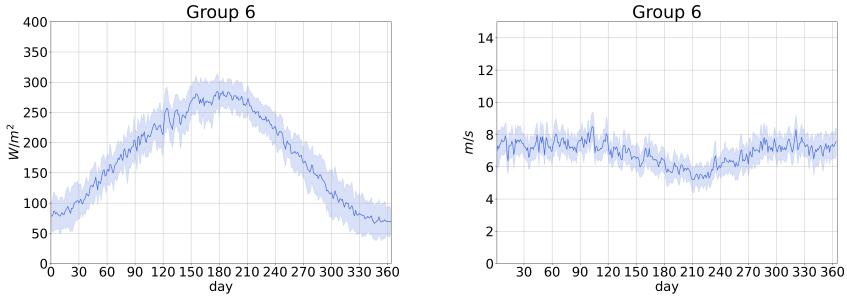

(b)

Figure 3.5: Climate data in a year of each group, (a) Group 4, (b) Group 6.

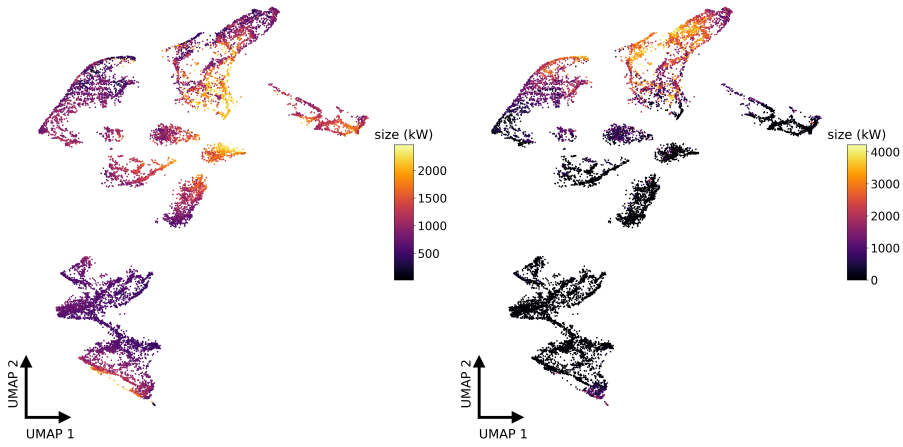

(a)

(b)

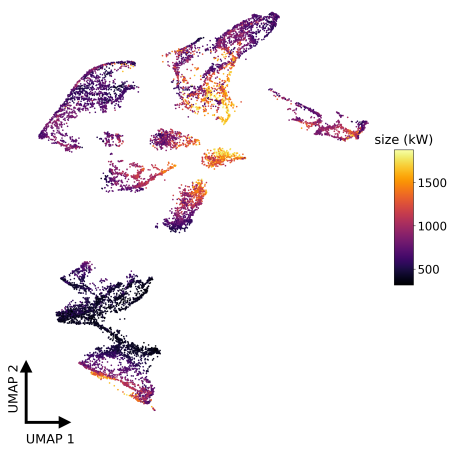

(c)

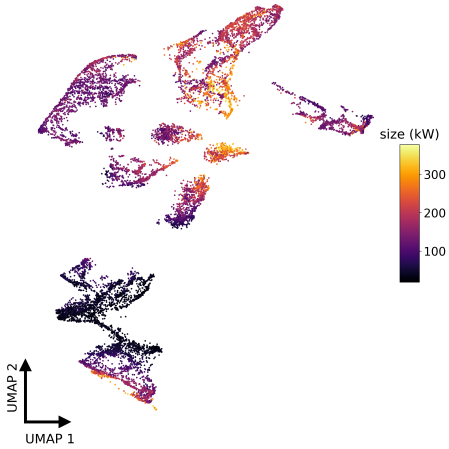

(d)

Figure 3.6: Optimal sizes of each unit mapped on the feature map of regional climate data, (a) PV module, (b) Wind turbine, (c) Electrolyzer, (d) Fuel cell.

3.3.2 Optimization of micro-grid considering climate variations

Letting project's life time 25 years, the sizes of a micro-grid system was optimized and the results are mapped on the feature map as shown in Fig 3.6. It was found that each cluster has the characteristic given by the optimal unit size. Each point in Fig. represents optimal unit size for each region as Fig. . As depicted in Figs. 3.6a and 3.6b, Groups 2 and 3 have dark points for wind turbines due to their small scale, whereas Group 9 has bright points for PV modules, indicating that it has large-scale units. Group 3 is also characterized by dark points for electrolyzer and fuel cell compared to the other groups (see Figs. 3.6c and 3.6d). While certain groups are distinguished by the size of each unit, regions in Group 4 and 6 exhibit a wide size variability, particularly for PV modules and wind turbines. This indicates that climatic conditions have a significant impact on the optimal unit sizes for Group 4 and 6, i.e., that they are sensitive to climate change.

Despite regions belonging to the same country, the form of optimal micro-grid is different since a climatic diversity exists in the country as mentioned in Section 3.3.1 Fig. 3.7 show 20 random samples from Groups 5 and 6 to investigate how optimal sizes were determined for each region. Most of the regions in both groups are located in the North America. Group 5 utilizes PV modules as their primary source of electricity, whilst Group 6 uses both types of generators. The regions with PV modules have wind turbines of relatively small size, and the unit sizes appear to have particular correlations. The unit sizes of the electrolyzer and fuel cell increase in proportion to the

size of the PV module as shown in Fig. 3.7a. Such a relationship between PV modules and other units has been identified as a significant component in the increase of the overall cost, as PV module and other unit sizes increase simultaneously. As illustrated in Fig. 3.7b, it is difficult to identify a trend in the sizes of the units in regions with wind turbines due to the simultaneous use of both electric generators. The results indicate that a design for micro-grid should consider climates in the region. To identify trends of optimal micro-grids regarding climatic patterns, the climatic characteristics and the optimization results of each group were compared.

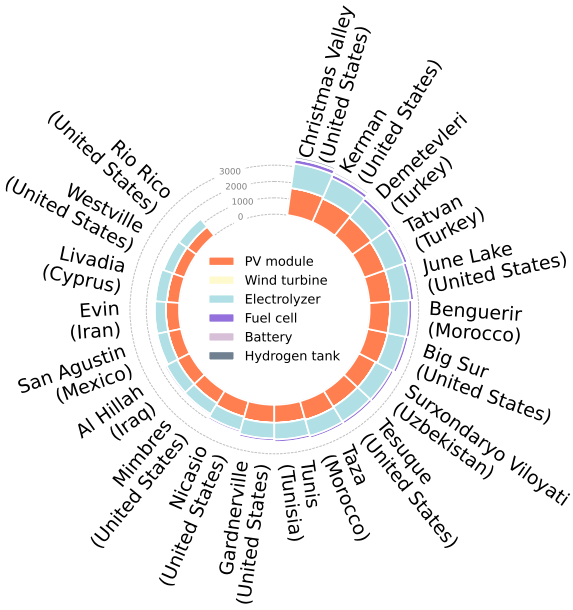

(a)

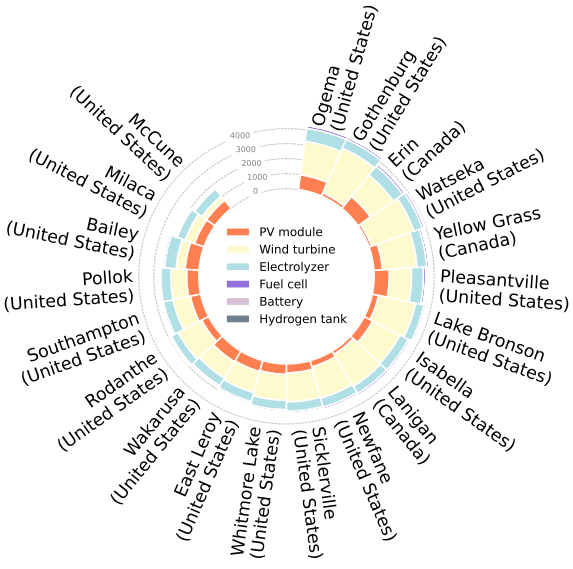

(b)

Figure 3.7: Unit sizes of 20 sample regions in each group, (a) Group 5, (b) Group 6.

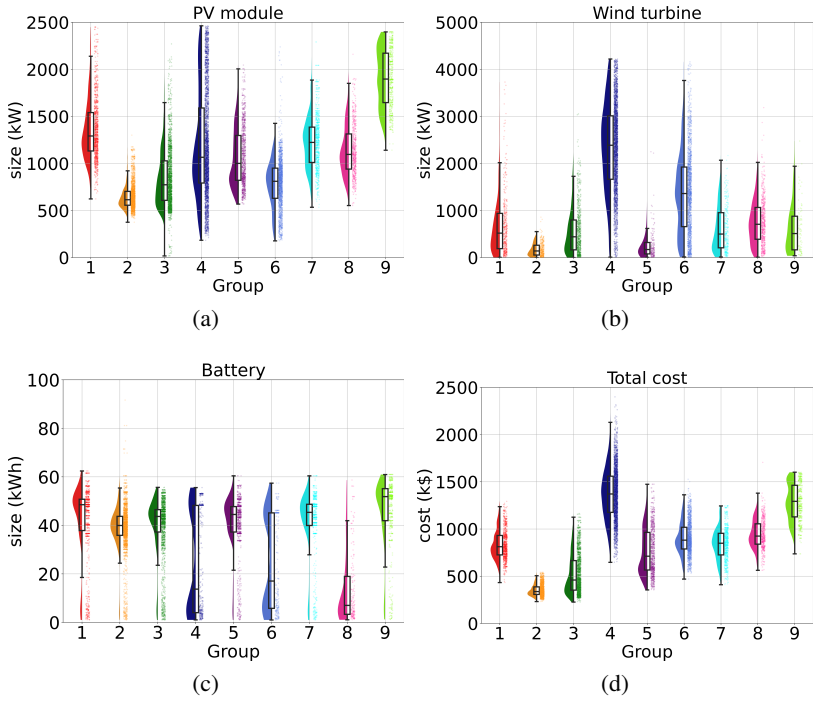

Figure 3.8: Optimization results, (a) optimal sizes of PV module (b) optimal sizes of wind turbine, (c) optimal sizes of battery, (d) total costs.

Table 3.4: Climate data in each group

group	Climate		
		irradiance (W/m^2)	wind speed (m/s)
1	mean	156.23	4.89
	standard deviation	25.46	1.04
2	mean	214.61	4.09
	standard deviation	32.83	1.50
3	mean	213.25	5.41
	standard deviation	39.57	1.53
4	mean	136.44	6.25
	standard deviation	24.06	1.27
5	mean	224.19	4.75
	standard deviation	25.55	1.06
6	mean	177.50	6.88
	standard deviation	28.34	0.79
7	mean	188.77	4.62
	standard deviation	20.03	0.80
8	mean	195.96	5.51
	standard deviation	16.73	0.84
9	mean	167.25	3.54
	standard deviation	19.74	0.76

The optimal size distribution of units in each group is depicted as a graph of rain clouds in Fig. 3.8. In the graph, the length of a rain cloud represents the variance of the distribution, and each rain cloud belongs to a distinct group. Only the distribution graph for optimal sizes of PV module, wind turbine, and battery and total cost in each group to be analyzed intensively is shown in Fig. 3.8, and overall distribution graphs are shown in the Appendix. There is a difference in the average size of each group and the wideness of the distribution also differs from each group. PV module and wind turbine are electric generators, and the optimization results of each group were substantially divided into two categories based on the electric generator that was mainly used. PV modules are the primary electric generator for Groups 1, 2, 3, 5, 7, and 9, while wind turbines are the primary generator for Groups 4, 6, and 8 (see Fig. 3.8a and 3.8b). Such a result appears to be a result of the variance in annual wind speed; the latter groups that use wind turbines as the main generator exhibit the highest annual wind speed (refer Table 3.4). The wind speeds of the former groups that use PV modules as the main generator are likewise determined to be below the cut-in speed. As shown in Fig. 3.8c, the battery unit is essential for the former groups. Solar power generation cannot be utilized when there is less sunlight (e.g., long night time or rainy season), so the comparatively large-sized battery serves as a buffer.

The optimal unit sizes are found to depend on climatic characteristics. The results of Groups 1, 5, and 7 indicate that the PV module size decreases as the yearly average irradiance increases. They have comparable yearly average wind speeds, around 4.7 m/s, but differing annual average irradiances.

Due to the rainy season, Group 1 has the lowest annual average irradiance at 156.23 W/m^2, followed by Group 7 at 188.77 W/m^2 and Group 5 at 224.19 W/m^2, the highest value among them. The optimal size of PV module was smaller in the order of Groups 5, 7, and 1 (see Fig. 3.8a and Table 3.4), indicating an inverse relationship between yearly average irradiance and PV module size.

When there is no significant difference between yearly average irradiance, the annual irradiance difference has a bigger impact on optimal size for Groups 2 and 5 than for the average. The average annual irradiance is larger in Group 5, but the sizes of PV module are also larger (see Fig. 3.8a and Table 3.4). As illustrated in Fig. 3.4b and 3.4d, the reason for this result was determined to be the yearly irradiance difference. If annual irradiance is nearly constant, PV modules provide electricity consistently. Otherwise, if irradiance varies over the course of a year, PV modules cannot match load needs when irradiance is low. In order to generate sufficient power even during periods of low irradiance, the optimal size of PV modules should be increased. In terms of cost, the larger the PV module size and the greater the cost, the lower the yearly average and the greater the annual variance. Group 2 had the lowest annual difference and the highest average annual irradiance, resulting in the lowest total cost as shown in Fig. 3.8d.

In certain regions, it is possible to avoid the optimal size of PV module from becoming excessively large by adding wind energy. In accordance with Fig. 3.8a and Table 3.4, the optimal PV module sizes for Group 9 are greater than those for Group 5, validating the above study, i.e., the lower the yearly average irradiance, the larger the PV module size. Group 9 should employ

PV modules that are twice as large as Group 5 due to their lower annual irradiation and wind speed. In particular, the wind turbine cannot be used as a power generator due to the low wind speed. Despite the lower annual irradiance, the optimal PV module dimensions for Group 8 are comparable to those for Group 5. This is because the wind turbine was utilized to subsidize solar energy production in Group 8. In lieu of increasing the size of the PV module, efficient power generation was achieved by installing a wind turbine of the same size. As shown in Table 2.1, wind turbines are less expensive than PV modules, and Fig. 3.8d demonstrates that the total costs of Group 9 were significantly higher than those of Group 5, whereas the total costs of Group 8 were comparable to those of Group 5, indicating that the costs of micro-grids in Group 8 were economical. Group 8 includes Spain and Italy, which are favorable regions for hybrid power generation.

When a wind turbine is employed as the primary electric generator, overall sizes of micro-grid are susceptible to climate change and the total cost of micro-grid is likely to be significant. As indicated in Table 3.4, the wind speeds in Groups 4 and 6 are the highest, and a wind turbine was chosen as the primary power generator for those groups. Since the power output of wind turbines is nonlinear to wind speed (see Equation 2.2), wind speed has a considerable effect on the sizes of wind turbines in Group 4 and 6, which have a wide range of sizes. In particular, the average size of the wind turbines in Group 4 was greater than that of the other groups, and the largest wind turbine was also included in Group 4 to supplement the insufficient solar power generation due to the lowest annual average irradiance, 136.44 W/m^2, as shown in Fig. 3.8b and Table 3.4. Consequently, the utilization of

a wind turbine is contingent upon both wind speed and irradiance. Additionally, wind speed impacts the size of a PV module in Group 4. PV module becomes a primary power generator when wind power is inefficient, and wind speed of Group 4 lies on the boundary between efficient and inefficient wind power, resulting in a wide range of PV module sizes. The total costs for Group 4 were the highest as shown in Fig. 3.8d. The results indicate that micro-grid, which relies mainly on wind power due to low irradiance, is economically inefficient.

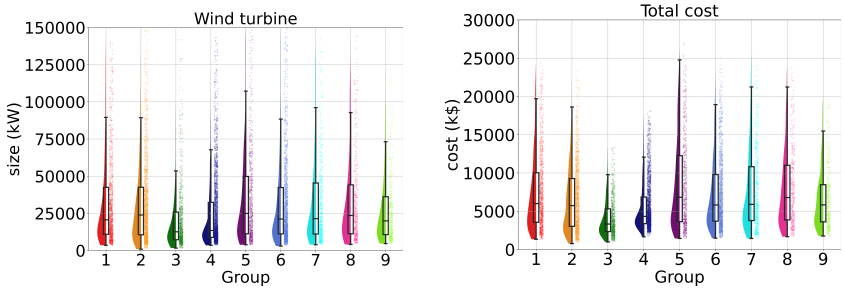

(a)

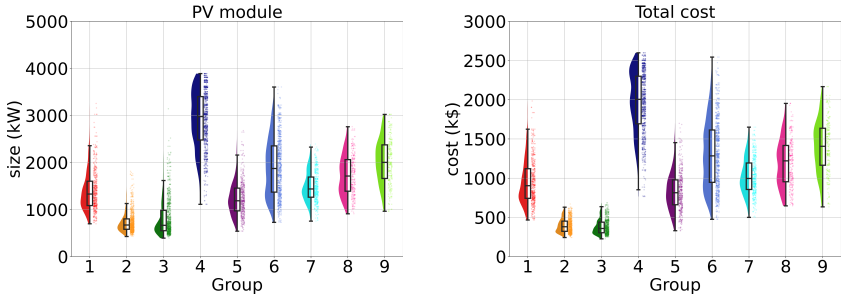

(b)

Figure 3.9: Optimization results for a single type of power generator, (a) a case using only wind turbine, (b) a case using only PV module.

Assuming a single type of power generator rather than a hybrid, i.e., PV module or wind turbine, optimization was performed and compared to a hybrid micro-grid. When a wind turbine is an unique power generator, every group has a large variance of sizes in wind turbines as well as total costs (see Fig. 3.9a). Resulting in similar optimal designs across the entire groups, the sizes of wind turbines exceed up to 75,000kW and the total costs are more than up to 20,000k$, which also indicates that a micro-grid based solely on a wind turbine is uneconomical. As shown in Fig. 3.9b, a micro-grid only utilizing a PV module is similar to a hybrid micro-grid except for Group 4 and 6. Groups 4 and 6 are climatically inefficient to rely solely on PV modules. Group 8 also has larger sizes in PV modules and higher total costs than hybrid cases since wind turbines do not exist as auxiliary power generators. The other groups, which mainly depends on PV modules in the cases of a hybrid micro-grid, shows similar sizes in PV modules and total costs. Through these two scenarios, it was confirmed that climatic characteristics of the region should be considered and the design of a micro-grid suitable for climates is necessary.

3.3.2.1 Intensive analysis for South Korea's climate and optimal results

As aforementioned, Group 1 has a distinctive pattern in the annual irradiance and South Korea's regions have also the pattern. However, not all regions in South Korea fall into Group 1, and two regions in South Korea are included in Group 6: Busan and Jeju. To identify factors that divided the two

regions and the other regions in South Korea into different groups, the climate of the Korean region belonging to Groups 1 and 6 was compared with the climate of the other regions. Figure 3.10 shows results of comparing the climate of South Korean regions in Group 1 and other regions in Groups 1 and 6. Both patterns of irradiance and wind speed of South Korean regions in Group 1 are more close to those of Group 1 than Group 6. On the other hand, in the case of South Korean regions in Group 6, pattern of irradiance is more close to that of Group 1 than Group 6, whereas pattern of wind speed is more similar to that of Group 6 than Group 1 as shown in Figure 3.11. Since irradiance pattern of Busan and Jeju is similar to Group 1, not Group 6, the factor that made the two regions belong to Group 6 is the pattern of wind speed. Normalized root mean square error (NRMSE) metric was used to numerically confirm the degree of similarity between the climates. As indicated in Tables 3.5 and 3.6, for South Korean regions in Group 1, both NRMSE values compared to other regions in Group 1 are smaller than those compared to other regions in Group 6, resulting the regions fall into Group 1. For South Korean regions in Group 6, however, NRMSE value of irradiance compared to other regions in Group 1 is smaller than that compared to other regions in Group 6, whereas NRMSE value of wind speed is the opposite. Nevertheless, difference of NRMSE value of wind speed compared to other regions in Group 1 is much larger than that compared to other regions in Group 6, and hence, the regions fall into Group 6.

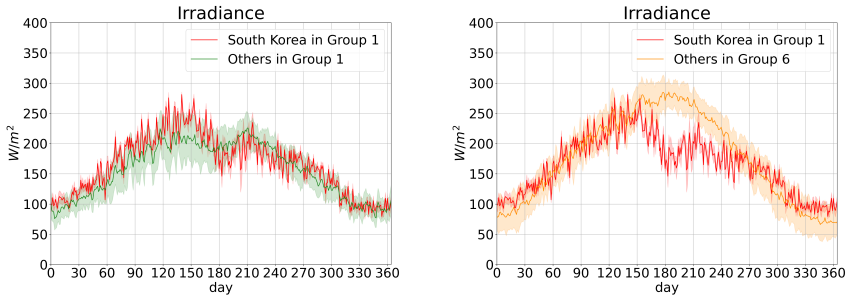

(a)

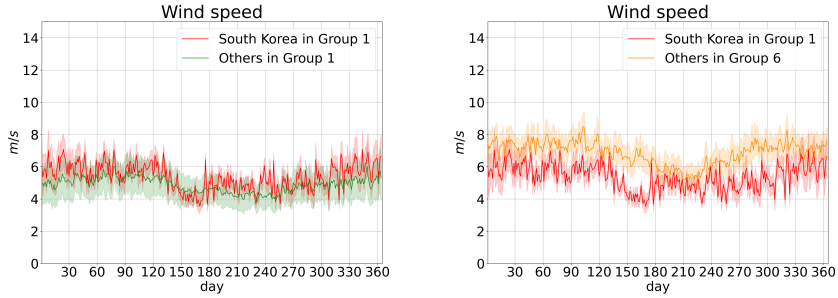

(b)

Figure 3.10: Climate of South Korean regions in Group 1 and other regions in Groups 1 and 6, (a) irradiance, (b) wind speed.

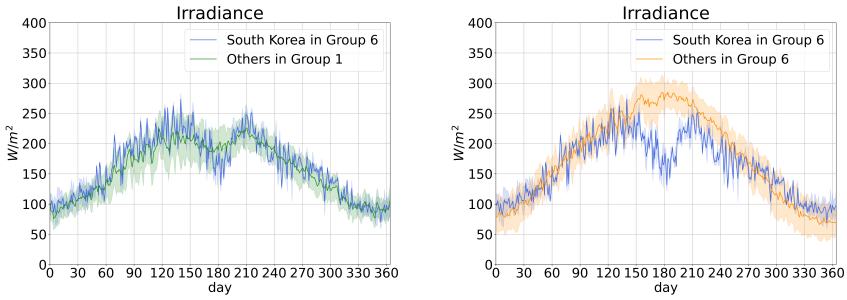

(a)

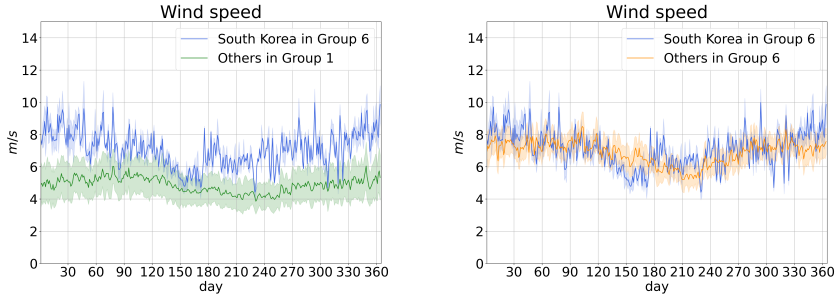

(b)

Figure 3.11: Climate of South Korean regions in Group 6 and other regions in Groups 1 and 6, (a) irradiance, (b) wind speed.

Table 3.5: Normalized root mean square error of irradiance.

		South Korea	
		Group 1	Group 6
Other regions	Group 1	3.04	3.56
	Group 6	6.71	9.66

Table 3.6: Normalized root mean square error of wind speed.

		South Korea	
		Group 1	Group 6
Other regions	Group 1	2.51	3.51
	Group 6	21.04	5.87

Based on the results of comparing climate data, we investigated the results of South Korean techno-economic analysis. First, in the case of Group 1, the average annual irradiance is high, thus the size of the PV module is smaller than the average in other regions. The average annual wind speed is also high, but it is still not economical to use wind power, and most of them focus on solar power generation. However, the sizes of the equipment or the total cost is almost on the average of other regions, These results indicate that the corresponding South Korean regions have typical climates of Group 1, resulting the regions have typical micro-grid structures. Next, in the case of Group 6, the average annual irradiance in South Korea is lower, but the average annual wind speed is higher than the other regions. Since the average annual irradiance is lower, the size of the PV module should be increased, however, higher wind speed induces sufficient wind power generation that compensates for this and prevent PV module from enlarging. Moreover, since wind power is proportional to the cube of the wind speed, it is possible to generate sufficient power with smaller wind turbine, and overall cost is also less compared to the other regions. As a result, South Korean regions of Group 6 are able to design and operate micro-grids that are economically advantageous.

3.3.3 Sensitivity analysis on the optimal unit sizes to climate variability

Variations in irradiance and wind speed were subjected to a sensitivity analysis to determine their effect on the optimal sizes of process units.

In general, sensitivity analysis is conducted for both positive and negative input variable changes. However, after completing sensitivity analysis, input changes in the opposite direction only result in output changes with the opposite sign, and the sensitivity scale is similar in both directions. Consequently, it would require a long analysis with comparable explanations to demonstrate all four outcomes: irradiance increase, irradiance decrease, wind speed increase, and wind speed decrease. Instead of using these typical climate changes, the actual climate changes of each group were taken into account for sensitivity analysis, and the results are anticipated to provide realistically applicable information for planning and operating the P2G process.

Based on 11 years of climate data from 2010 to 2020 for each group, the amount and direction of climate change were determined. The standard deviation of yearly irrandiance and wind speed was calculated, and climates were shifted by 10% of the standard deviation. The direction of the change was determined by the trend of climate changes over 11 years; for example, the climate was shifted in a negative direction if the trend line of the average annual climate for 11 years derived using linear regression slopes downward. Table 3.7 displays the magnitude and direction of climate change for each group. On the basis of the shifted climates, the optimal sizes of process units in each group were determined and nine groups were classified into four types based on their sensitivity to climate change and the direction of the change: climate-sensitive with the same direction (Type S+), climate-sensitive with the opposite direction (Type S-), climate-insensitive with the same direction (Type I+), and climate-insensitive with the opposite direction

(Type I-). The term "climate-sensitive" refers to the sensitivity of optimal unit sizes to climate changes. Same direction shows that the annual irradiance and wind speed vary in the same direction, whereas opposite direction suggests the contrary. Table 3.7 shows which type each cluster belongs to. Climate change shift the optimal sizes of micro-grid, and a decrease in climate generally leads to an increase in unit size because, for instance, a larger PV module is required to generate sufficient power with reduced irradiance to meet both types of load demands. In this work, since the climate shift directions for each cluster are distinct, we analyzed sensitivity using the absolute value of the changes to compare the rates of changes in different directions.

Table 3.7: Shift ratio and direction of each group

group	Shift ratio (%)		Shift direction		Type
	irradiance	wind speed	irradiance	wind speed	
1	2.13	4.21	increase	decrease	I-
2	1.20	3.38	increase	decrease	I-
3	1.49	3.44	increase	decrease	I-
4	2.08	3.98	increase	increase	S+
5	1.10	4.27	increase	decrease	I-
6	1.86	3.91	decrease	decrease	S+
7	1.83	3.71	decrease	decrease	I+
8	1.38	4.55	increase	decrease	S-
9	1.71	4.62	increase	increase	I+

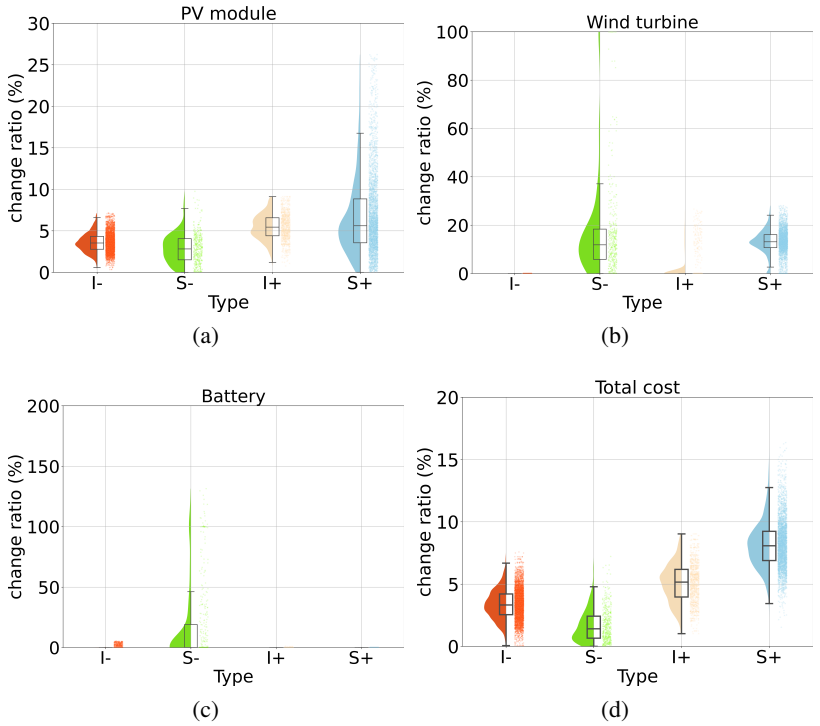

Figure 3.12: Sensitivity results, (a) PV module, (b) wind turbine, (c) battery, (d) total cost.

As shown in Fig. 3.12, Type I+/- exhibits less unit size variation than Type S+/-. When annual irradiance increases between 1.10–2.13% and annual wind speed falls between 3.38–4.27%, only the size of the PV module is reduced by 3.60±0.03% in Type I-. Type I+ demonstrates a change in PV module size of 5.46±0.08% and a modest change in wind turbine size of 2.02±0.28%. Therefore, the overall size of the micro-grid in Type +/- is insensitive to climate change because they did not deploy wind turbines or there was minimal change in wind turbines. In Type S+/-, however, the PV module and, in particular, the wind turbine were modified, leading in major modifications to the unit sizes of the process. Type S+ requires a 6.79±0.13% increase in PV module size and a 13.02±0.15% increase in wind turbine size when annual irradiance decreases between 1.86 and 2.08% and annual wind speed falls between 3.91 and 3.98%. As depicted in Fig. 3.12a and 3.12b, the modifications are two to four times that of the other categories. Moreover, while both the original unit sizes and the sensitivity to climate change in Type S+ were substantial, the adjustments to the scale were the most important. According to Tables 3.3 and 3.7, nations such as the United States and Canada are Type S+, therefore climate variability must be taken into account while developing and managing micro-grid systems.

Even though the size of the PV module and wind turbine changed by 2.91±0.14% and 17.90±1.74%, respectively, in Type S-, the total cost change was the smallest of all kinds, as shown in Fig. 3.12d. This is due to the fact that Type S- micro-grids employ a trade-off between PV modules and wind turbines to offset the overall changes, which other types of micro-

grids could not achieve. When the bulk of the annual wind speed falls below the cut-in wind speed, the wind turbine cannot generate sufficient and efficient power. Therefore, it is reasonable to replace wind turbines with photovoltaic modules as the primary source of energy. This trade-off is intensified when yearly irradiance increases. Sharp changes of the battery in Type S- indicate the existence of a trade-off (see Fig. 3.12c), as the battery is a necessary unit as a buffer when the PV module is the only power producer. The cost savings of wind turbines offset the cost increases of PV modules and batteries, resulting in the smallest rise in total cost. Due to the identical shift direction of annual irradiance and wind speed, the ratio of cost change was bigger in Type S+ and Type I+ regions than in Type S- and Type I- regions, indicating that the trade-off is unachievable. Due to the identical shift orientation and utilization of wind turbines, Type S+ has the greatest cost costs. Type I+ has fewer cost transitions than Type S+ due to the infrequent use of wind turbines, while Type I- has even fewer cost transitions because there is no change in wind turbine size (see Fig. 3.12b). Although cost-effective micro-grid systems can be attained through Type S- trade-offs, the abrupt differences in unit sizes make it difficult to identify a suitable design and to maintain it for years. Therefore, the Type S- regions should be handled with care. For example, when the battery is modularized in a structure consisting of small modules connected in series as opposed to one large module, it can accommodate both small and large battery cases. European regions near the Mediterranean are of Type S- as indicated in Table 3.3 and 3.7.

Chapter 4

Energy management and design of multi-stack micro-grid under climatic uncertainty

4.1 Introduction

The NOAA (National Oceanic and Atmospheric Administration) noted that Global temperatures have risen at a rate of 0.18 °C each decade since 1981, which is twice as fast as before and it was the second warmest year on record in 2019 [2, 3]. Due to the growing interest in the global climate crisis, research on power generation or power-to-gas using renewable energy has been implemented [4, 5] and research on the micro-grid utilizing renewable energy has increased [6]. Techno-economic analysis of a micro-grid has been investigated and the sizes of the equipment such as photovoltaic (PV) modules, electrolyzers, and fuel cells in a micro-grid have been optimized. For instance, the sizing problems for micro-grids that consist of PV module, wind turbine, diesel generator, electrolyzer, fuel cell, and a load have been solved [7, 8, 9]. A stand-alone micro-grid based on hybrid renewable energy sources has been optimized [10, 11, 12, 13, 14, 15]. Considering life-cycle cost, renewable energy penetration, and pollutant emission as the objective function, the sizes in a stand-alone micro-grid have been optimized

based on rule-based operation [16]. Research on energy management system (EMS) have been conducted to facilitate the efficient and secure operation of a micro-grid. EMS has been developed through model predictive control, dynamic programming, mixed-integer linear programming, and nonlinear programming [17]. In particular, EMS of a micro-grid with renewable energy sources has considered uncertainty of renewable energy due to variability and intermittent nature in the renewable energy. Two stage stochastic programming has been formulated based on scenario-method, considering optimal sizing and operations simultaneously [21]. With parameterized renewable power, optimal explicit rule has been obtained on off-line in advance to operate a micro-grid [19]. Energy management of a renewable micro-grid has been optimized using SAM-theta-PSO algorithm to consider uncertainty [20]. There are micro-grids composed of multi-stack equipment and their EMS has also been developed. A multi-stack micro-grid has advantage of reducing operation and management costs and saving lifetime of equipment via scheduling on and off of each stack. The usage of multi-stack fuel cells has been scheduled to minimize costs of equipment and meet load demands [22, 23, 24]. Different types of multiple batteries in a micro-grid have been operated to minimize battery life consumption and meet load demand [25]. It is necessary to consider a trade-off between economies of scale and efficiency of operations when deciding the number of stacks and their sizes. When equipment is divided into multiple stacks and a size of a stack becomes smaller, costs of equipment increase due to failure of economies of scale [26]. At the expense of economies of scale, a multi-stack micro-grid can be more economic through efficient operations especially when oper-

ating a micro-grid at best operating level. Operations of a micro-grid with renewable energy sources depend on climatic condition, thus the number of stacks and their sizes should be decided according to climatic influences for efficient operations and equipment's safety.

There have been studies on managing energy distributions for a micro-grid with robust or stochastic programming, which considers climate uncertainty. A robust optimization considered uncertainties of wind power to manage the mixture composed of hydrogen, liquid Petroleum gas, and Nitrogen and maximize hydrogen injection [27]. Adopting integer variables to describe on-off state of power generator and energy storage system, scenario based stochastic mix-integer linear programming has optimized the cost function [28, 29]. Adaptively constrained model predictive control for a micro-grid has been suggested with chance constraints for boundaries of state-of-charge in the battery [30]. Despite diverse approaches to handle uncertainty in a renewable micro-gird with stochastic optimization, there have been the lacks of research on a micro-grid with multi-stack units. In addition, few studies have considered climatic effects on design of multi-stack micro-grids and investigated relationships between economies of scale and efficiency of operations. Although a study has optimized cost by size of the battery and EMS of a hybrid renewable energy system at the same time using two-stage stochastic decision problem [59], a micro-grid was composed of single equipment and economies of scale were disregarded.

To address these issues, we suggest a novel mixed-integer stochastic programming (MISP) to simulate a multi-stack micro-grid under climate uncertainty. Stochastic optimization includes probabilistic constraints

which are transformed into a deterministic form with algorithms such as stochastic tube method, scenario-based method, and scenario-tree method [60]. When a micro-grid comprises multiple equipment, decision variables in EMS increase, thus it is improper to use scenario-based stochastic optimization or scenario-tree method which already conducts scenario reduction algorithms to decrease computational burdens [61]. Therefore, MISP in this paper was formulated using stochastic tube method to prevent computational costs from enlarging excessively. We evaluate performance of the proposed method compared to mixed-integer programming which is unconcerned about uncertainty. To analyze a trade-off between economies of scale and efficiency of operations under climatic variability, design of multi-stack micro-grids were determined via grid-search among the candidates using real climate data and the suggested MISP. Through this approach, we validated the better performance of the suggested MISP for a multi-stack micro-grid, confirmed importance of considering climatic variability when a design of renewable micro-grid covers multiple stacks of equipment, designed multi-stack micro-grids in two different cities, and verified climatic effects on the trade-off.

In Section 4.2.1, modeling and stochastic programming for a multi-stack micro-grid system were formulated, and we figured out regional climatic variability influence the trade-off between economies of scale and efficiency of operations in Section 4.3.1

4.2 Method

4.2.1 Objective function

Although the project's lifetime in the techno-economic analysis of a micro-grid is over 20 years, operating time in our EMS is in hours, thus the costs are converted to an hourly rate instead of using the annualized costs.

EMS performs on-off scheduling to make a micro-grid costly efficient, reducing O&M costs and delaying replacements of units. The cost saving operation is accomplished through reflecting ratio of actual operated time to the entire period on the O&M cost, replacement cost, and salvage value with binary variables which indicates the on-off state of each unit. Thus Equation 2.7 is modified as:

$$
\begin{aligned}
NPC &= C_{cap} + \sum_{n=1}^{N} i_d \cdot C_{OM} \frac{z_n}{N} + i_d^N \left(C_{rep} Integer \left(\frac{\sum_{n=1}^{N} z_n}{Rep} \right) - S \right) \\
S &= C_{rep} \frac{Rem}{Rep} \\
i_d &= \frac{1}{(1+i_r)^n} \\
i_d^N &= \frac{1}{(1+i_r)^N} \\
i_r &= \frac{i_n - f}{1+f}
\end{aligned}
\tag{4.1}
$$

where z_n denotes the on-off state of each unit at time n.

In addition, economies of scale should be considered when a single unit is divided into multi-stacked unit. The costs for multi-stacked units are

measured using the ".6 rule" as a capacity of each unit decreases [26].

$$\frac{C_2}{C_1} = \left(\frac{X_2}{X_1}\right)^{0.6} \tag{4.2}$$

where C_1 and C_2 are the costs of two units and X_1 and X_2 are the capacities of them respectively.

4.2.2 Irradiance and load demands

For simulation of EMS, irradiance data in Washinton, United States consist of hourly data with about 4000 days from 2010 to 2020 and were collected from the Prediction of Worldwide Energy Resource (POWER) Project's Hourly 2.0.0 version on 2022/01/21 [47]. Randomly selected dates compose irradiance scenario that is assumed as real irradiance distribution. As the prediction data, 1000 pieces of data similar to the real irradiance observed up to the present are estimated and one of them is randomly selected at every time step. Fig. 4.1 shows an instance of real and predicted irradiance. Global climate data were gathered from the Prediction of Worldwide Energy Resource (POWER) Project's Hourly 2.0.0 version on 2022/01/21. [47]. For design of hybrid micro-grids with PV module and wind turbine, we collected irradiance and wind speed data for 8,760 hours by scraping open sources in National Aeronautics and Space Administration (NASA) Langley Research Center and implemented clustering based on the data. Electricity and hydrogen load requirements were taken into account. In general, their values are described as random variables whose patterns include a decrease at night and an increase during the day. The load requirements were arbi-

trarily generated by adding white noise to a sine function for simulations. The range of the electricity load demand was between 0.5 and 5 kW/hr and the range of the hydrogen load demand was between 1 and 2 kg/hr.

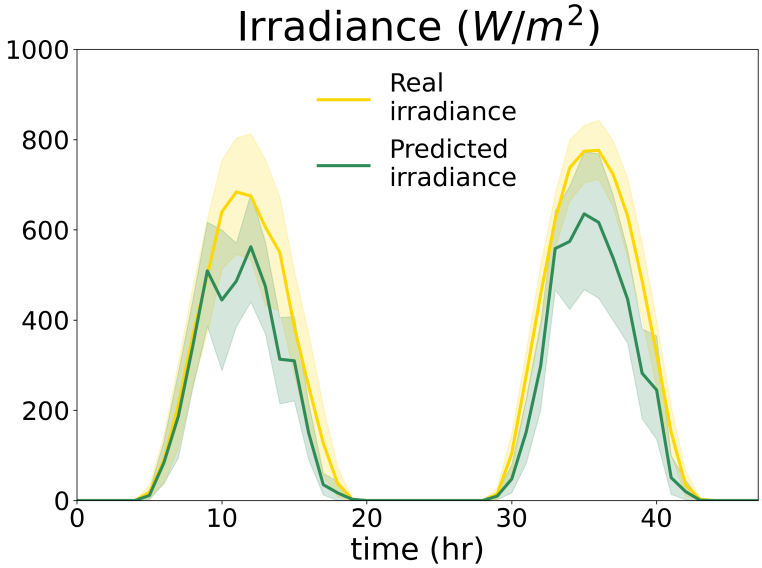

Figure 4.1: Real irradiance and predicted irradiance.

4.2.3 Mixed-integer stochastic programming for a multi-stack micro-grid

Assuming equipment of a micro-grid consist of multiple stacks except for PV module, modeling was implemented for on-off scheduling of the micro-grid. Suggested model includes binary variables for each unit's on-off state and continuous variables for power and hydrogen flows and control inputs, which means mixed-integer formulation. State of a micro-grid is the ratio of charged power in each battery to its capacity and the ratio of the volume of stored hydrogen to the tank's size. Batteries have a role to buffer power generated from PV module, thus the power flows from PV module to battery at first and is delivered to other units by discharging the battery. While battery's SoC is fluctuated through charging from PV module and fuel cell and discharging to electrolyzer and electricity load, hydrogen tank stores hydrogen produced from electrolyzer and releases it to fuel cell and hydrogen load.

$$
\begin{aligned}
dP^i_{ba,t} &= P^i_{pv,t} + \sum_{l=1}^{N_{fc}} P^{il}_{fc,t} - \sum_{k=1}^{N_{ez}} P^{ik}_{ez,t} - P^i_{el,t} \\
SoC^i_{t+1} &= SoC^i_t + \frac{\eta_{ba}}{C^i} dP^i_{ba,t} \\
\forall i &\in 1, ..., N_{ba}
\end{aligned}
\tag{4.3}
$$

$$
\begin{aligned}
d\dot{H}_{2_t}^{\ j} &= \sum_{k=1}^{N_{ez}} \dot{H}_{2_{ez,t}}^{\ jk} - \dot{H}_{2_{hl,t}}^{\ j} - \sum_{l=1}^{N_{fc}} \dot{H}_{2_{fc,t}}^{\ jl} \\
SoH_{t+1}^{j} &= SoH_t^j + \frac{\eta_{ht}}{C_{H_2}^j} d\dot{H}_{2_t}^{\ j}
\end{aligned} \tag{4.4}
$$

$$\forall j \in 1, ..., N_{ht}$$

The power consumption of electrolyzer and power generated from fuel cell are limited by equipment's size and powers should be zero if the equipment is off. Consequently, the optimization problem for on-off scheduling is formulated as follows:

$$
\begin{aligned}
&\min E\,[\textit{NPC in Equation 4.1}] \\
\textit{s.t.}\quad &\textit{model in Equations 2.1-2.4 and 4.3-4.4} \\
&SoC_{min} \leq SoC_t^i \leq SoC_{max} \\
&SoH_{min} \leq SoH_t^i \leq SoH_{max} \\
&-z_{ba,t}^i M \leq dP_t^i \leq z_{ba,t}^i M \\
&-z_{ht,t}^j M \leq d\dot{H}_{2_t}^{\ j} \leq z_{ht,t}^j M \\
&\forall i \in 1, ..., N_{ba} \\
&\forall j \in 1, ..., N_{ht} \\
&P_{el,t}^{sp} - \epsilon \leq \sum_{i=1}^{N_{ba}} P_{el,t}^i \leq P_{el,t}^{sp} + \epsilon \\
&\dot{H}_{2_{hl,t}}^{\ sp} - \epsilon \leq \sum_{j=1}^{N_{ht}} \dot{H}_{2_{hl,t}}^{\ j} \leq \dot{H}_{2_{hl,t}}^{\ sp} + \epsilon
\end{aligned} \tag{4.5}
$$

where $z^i_{ba,t}$ and $z^j_{ht,t}$ are binary variables that denote the on-off state of battery and hydrogen tank respectively, and SoC_{min} and SoC_{max} represents the minimum and maximum values of SoC, SoH_{min} and SoH_{max} represents the minimum and maximum values of SoH, $P^{sp}_{el,t}$ and $\dot{H}^{sp}_{2hl,t}$ are the load demands of electricity and hydrogen at time t, and M is a large positive real value for big-M method.

Since uncertainty of irradiance makes PV module's power output stochastic, it directly influences SoC of each battery. Converting boundaries of SoC in Equation 4.5 to chance constraints, Equation 4.5 becomes stochastic programming to handle the uncertainty. The chance constraints that satisfies the boundaries with a probability of 1-β is as follows.

$$Pr\left[SoC_{min} \leq SoC^i_t \leq SoC_{max}\right] \geq 1-\beta, \quad \forall i \in 1, ..., N_{ba} \tag{4.6}$$

To relieve correlations between chance constraints of SoC, $P^i_{pv,t}$ is assumed as independent and identically distributed random variable (i.i.d.). Still, the chance constraint for each battery in Equation 4.6 is a joint chance constraint, thus stochastic tube method is inapplicable. The joint chance constraints were relaxed into single chance constraints using Bonferroni inequality.

$$\begin{aligned} &Pr\left[SoC_{min} \leq SoC^i_t \leq SoC_{max}\right] \\ &\geq Pr\left[SoC^i_t \geq SoC_{min}\right] + Pr\left[SoC^i_t \leq SoC_{max}\right] - 1 \end{aligned}$$

Therefore, Equation 4.6 is satisfied if the following equation is satis-

fied:

$$Pr\left[SoC_t^i \geq SoC_{min}\right] + Pr\left[SoC_t^i \leq SoC_{max}\right] \geq 2 - \beta \quad \forall i \in 1, ..., N_{ba} \tag{4.7}$$

and Equation 4.7 can be divided into two inequalities, converting a joint chance constraint into two single chance constraints.

$$\begin{aligned} Pr\left[SoC_t^i \geq SoC_{min}\right] &\geq 1 - \beta_1 \\ Pr\left[SoC_t^i \leq SoC_{max}\right] &\geq 1 - \beta_2 \\ \beta = \beta_1 + \beta_2, \quad \forall i \in 1, ..., N_{ba} & \end{aligned} \tag{4.8}$$

$P_{pv,t}^i$ must be zero mean random variables in order to use stochastic tube method, thus $P_{pv,t}^i$ is substracted by its expectation value. Since $P_{pv,t}^i$ is assumed as i.i.d., expectation of $P_{pv,t}^i$ equals to fraction of the expected whole PV module's power output which is the averaged values obtained through Monte Carlo sampling based on real climate data set.

$$\begin{aligned} \hat{P}_{pv,t}^i &= \alpha_t^i \hat{P}_{pv,t} \\ \hat{P}_{pv,t} &= \frac{1}{N_s} \sum_{s=1}^{N_s} P_{pv,t,s} \\ \tilde{P}_{pv,t}^i &:= P_{pv,t}^i - \hat{P}_{pv,t}^i \end{aligned} \tag{4.9}$$

where $\hat{P}_{pv,t}^i$ and $\hat{P}_{pv,t}$ represent the averages of $P_{pv,t}^i$ and $P_{pv,t}$, $\tilde{P}_{pv,t}^i$ represents the error of $P_{pv,t}^i$ that is a zero mean random variable, and N_s is the

number of samples for Monte Carlo sampling.

According to stochastic tube method, Equation 4.9 is reformulated to hard constraints with inverse cumulative density functions of $\tilde{P}^i_{pv,t}$ as:

$$\begin{aligned} Pr\left[SoC^i_t \geq SoC_{min}\right] &\geq 1-\beta_1 \\ \Rightarrow SoC_{min} - SoC^i_t &\leq F^{-1}(\beta_1) \end{aligned}$$

$$\begin{aligned} Pr\left[SoC^i_t \leq SoC_{max}\right] &\geq 1-\beta_2 \\ \Rightarrow SoC_{max} - SoC^i_t &\geq F^{-1}(1-\beta_2) \end{aligned}$$

where F is the cumulative density function of $\tilde{P}^i_{pv,t}$.

$F^{-1}(\beta_1)$ and $F^{-1}(1-\beta_2)$ are decided by the approximated inverse cumulative density function through Monte Carlo sampling as shown in Fig. 4.2.

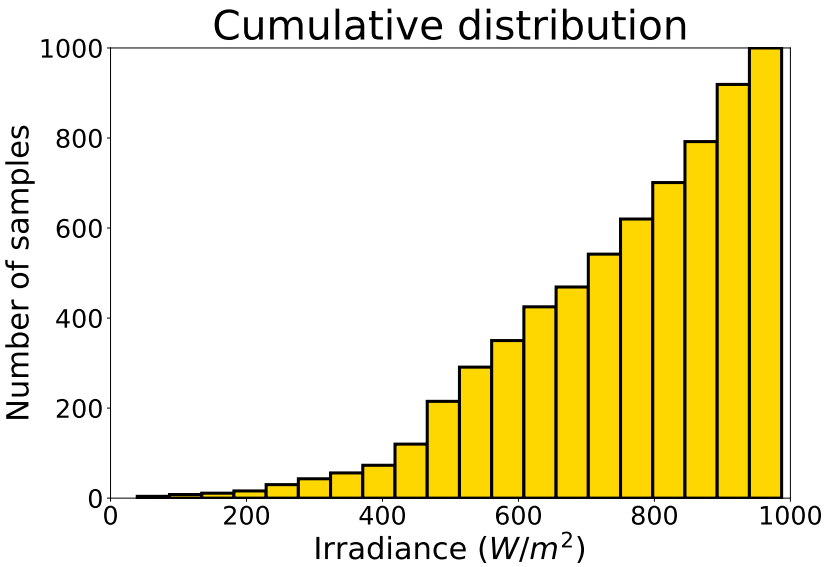

Figure 4.2: Cumulative distribution function of irradiance.

4.3 Result and discussion

4.3.1 Size decision of a multi-stack micro-grid under climate uncertainty

A multi-stack micro-grid is operated at a best operating level based on EMS with MISP, thus a trade-off between economies of scale and effective operations is considered to determine the number of stacks and their sizes. For case study, total sizes of process units are given as 500kW for a PV module, 2000kW for an eletrolyzer, 1000kW for a fuel cell, 2000kWh for a battery, and 1000kg for a hydrogen tank. It is assume that each unit except PV module can be divided into maximum 4 parts, i.e., a large single unit, two units of 3:1 or 1:1, three units of 2:1:1, and four equal size units. The costs of small size stacks are calculated with Equation 4.2 based on the total sizes. Since each equipment has 5 types and there are four kinds of equipment in a micro-grid, the total number of possible micro-grid's types is 625. Simulating each type of micro-grid for 10 iterations, the most economic type is selected among them. In addition, simulations were conducted and their results were compared based on data from two different regions in order to verify the influence of climatic patterns on the trade-off between economies of scale and effective operations.

Table 4.1: Specifications of multi-stack micro-grid

	PV module	Electrolyzer	Fuel cell	Battery	Hydrogen tank
Pingliang, China	500 kW	500 kW	500 kW	1500 kWh	500 kg
		500 kW			
		500 kW	250 kW		250 kg
		500 kW	250 kW	500 kWh	250 kg
San Bernardino, United States	500 kW	500 kW	500 kW	1000 kWh	250 kg
		500 kW			250 kg
		500 kW	250 kW	500 kWh	250 kg
		500 kW	250 kW	500 kWh	250 kg

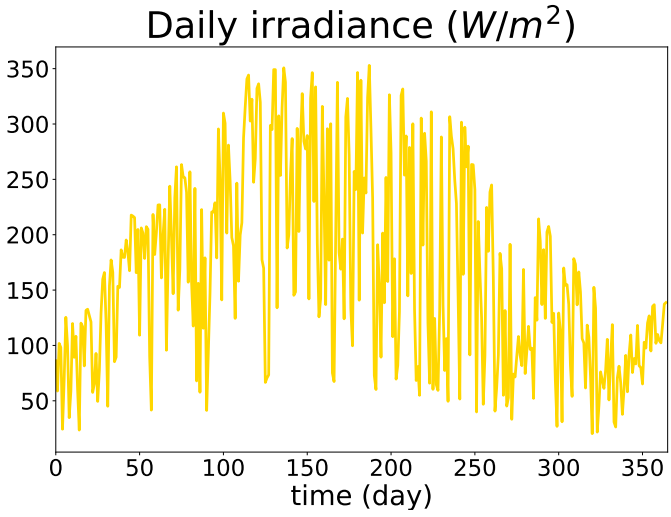

(a)

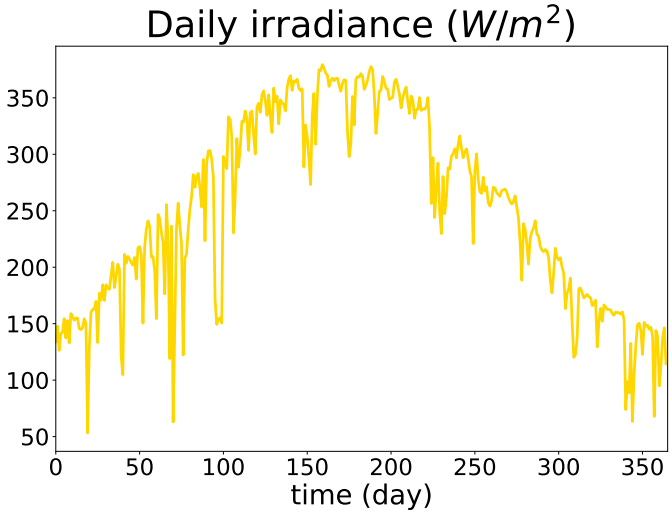

(b)

Figure 4.3: Daily irradiance, (a) Pingliang in China, (b) San Bernardino in United States.

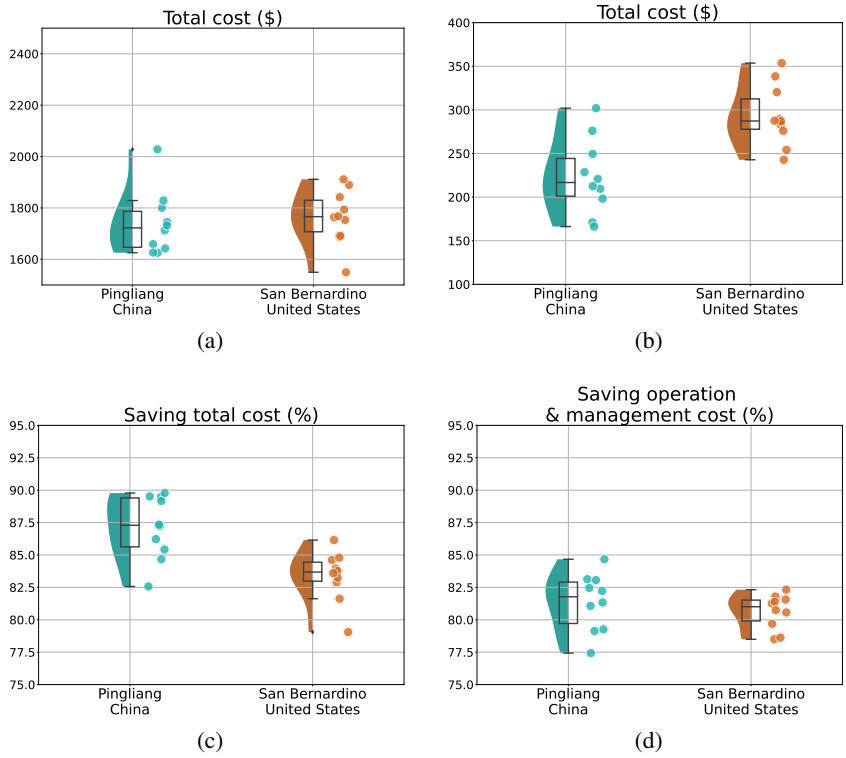

Figure 4.4: size decision of multi-stack micro-grids in two regions, (a) Total cost for single unit micro-grids, (b) Total cost for multi-stack micro-grids, (c) Ratio of saving total cost for multi-stack micro-grids, (d) Ratio of saving operation and management cost for multi-stack micro-grids.

As shown in Fig. 4.3, irradiance data from Pingliang in China and San Bernardino in United States were used to find the most economic multi-stack structure, and their climate are different noticeably. Pingliang in China has a more intermittent irradiance than San Bernardino in United States. The total cost of a single unit micro-grid for each region is shown as in Fig. 4.4a and similar each other with slight dispersion. Through a grid search across 625 candidates, the minimum multi-stack structure at every iteration was determined and their distributions of total cost are shown in Fig. 4.4b and the structure was indicated in Table 4.1. A multi-stack micro-grid in Pingliang has less divided structure, thus has the advantage of economies of scale.

In spite of the initial similar distribution, the total cost of optimal structure was different in each region, which means climatic characteristics affects a trade-off between economies of scale and advantages of flexible operations. Fig. 4.4c indicates that a multi-stack micro-grid under climate of Pingliang in China achieved more economical benefits from separating equipment into multi-stacks. Comparing cost saving ratio, while the micro-grid in San Bernardino still saved more than 80%, the micro-grid in Pingliang cut down expenses almost 90%, and 1-quantile of total cost of Pinglinag's micro-grid is higher than 3-quantile of that of San Bernardino's micro-grid.

Nonetheless, the micro-grid in Pingliang did not achieve the economic strategy from efficient scheduling. Cost saving ratios by operations are similar in both micro-grids, indicating the micro-grid in San Bernardino surmounted economies of scale via more flexible scheduling (see Fig. 4.4d). Variance of cost saving ratio by operations in Pingliang is larger than that

in San Bernardino due to climate variability. Although two regions saved operating costs at the similar level, economies of scale made the micro-grid in Pingliang save more total cost. Still, two regions attained more than 80% of cost saving in average, and we confirmed economic advantages of multi-stack micro-grids regarding to single unit micro-grids. In addition, climatic variability has a considerable influence on design of a multi-stack micro-grid.

Chapter 5

Concluding remarks

Plentiful renewable energy sources are essential to construct, operate, and manage renewable energy micro-grids, and the amount of renewable energy has an intermittent nature, therefore, climatic variability is a pivotal issue for a micro-grid system. Nonetheless, previous studies have rarely investigated influences of climatic variability on techno-economic analysis of a micro-grid, and size decision and energy management of a multi-stack micro-grid. Big data driven analysis and mixed-integer stochastic energy management are exploited to resolve these limitations.

The special features can be written as follows: First, the correlation analysis through unsupervised clustering is carried out to verify that climatic variability is a factor that determine the design of techno-economical micro-grids. Mitigating their noise and clustering them via UMAP and HDBSCAN algorithm, climate data from 13,844 cities in 218 nations are used to the correlation analysis. Second, the strategies to install and operate a micro-grid during long project's lifespan are suggested according to regional climatic features. In third, a mixed-integer stochastic programming is developed to control a multi-stack micro-grid's energy distributions. Finally, it is verified

that the climatic effects are noticeable in design of a multi-stack micro-grid.

5.1 Summary of the contributions

In this thesis, strategies for design of a micro-grid are discussed to suggest techno-economical structures and operations under climate variability. The climate data are gathered from the Prediction of Worldwide Energy Resource (POWER) Project's Hourly 2.0.0 version on 2022/01/21, which means is relevant to the actual design of P2G systems.

The first part is to analyze techno-economical micro-grid systems via unsupervised clustering. Climate-similar locations are clustered and their optimal structures of micro-grids have characteristic depending on the climatic patterns. While some locations are aparted from, but still in the same group due to similar latitude, others are classified into different groups despite being nearby, and their optimal designs are also disparate. It is verified that techno-economical micro-grids are correlated to climatic patters across clustered regions via unsupervised learning. According to sensitivity analysis, we clarify that the majority of the locations surrounding the equator, the Far East, and the Southern Hemisphere, including China, India, Mexico, and Brazil are insensitive to climatic pattern changes, thus have an advantageous of operating renewable micro-grids. Meanwhile, regions in the high latitudes of the Northern Hemisphere, including 1,890 regions in the United States, Canada, and Russia, are the most sensitive to climate changes, and hence should be cautious about climate change. The strategies for design of a micro-grid are established for actual countries and directly applicable to

the actual design of P2G systems.

In the second part, we decide the structures of multi-stack micro-grids in the presence of climatic variability. There is a trade-off between economies of scale and efficiency of operations and climatic variability is inevitable part of operating a micro-grid efficiently. We suggested the mixed-integer stochastic programming for multi-stack micro-grids since few researches have investigated to control the micro-grids under climate uncertainty. Relaxing joint chance constraint and assuming that climate uncertainty is zero mean, independent, and identically distributed random variables, the suggested method successfully manages the energy distributions of the micro-grids as illustrated via a case study. Based on the suggested method, case study is conducted to find a suitable multi-stack structure in two regions. In the climate of Pingliang, China, micro-grids have more economic benefits with fewer stacks than micro-grids in the climate of the San Bernardino, United States. As a consequence, we identified that the designs of multi-stack micro-grids are related to climatic variability.

5.2 Future works

The overall analyses are restricted to linear micro-grid models and the assumptions such as deterministic load demands, no degradation of equipment, and ambient temperature. Even though the linear models and such assumption are widely exploited in the techno-economic analysis fields, it is still less realistic to limit micro-grid models into the simplified settings. Nonetheless, it is rational to use the simple models since big data analysis is

fatal to nonlinear models which send computational costs soaring. Utilizing linear models, computational efficiency is secured for big data analysis in Section 3.3.2 and grid search in Section 4.3.1, Still, despite the feasonable choice, it is necessary to make an effort to apply the nonlinear model in order to increase the realities of the analyses. Therefore, future works should propose a more realistic analysis by constructing mixed-integer nonlinear programming rather than mixed-integer linear programming. Accordingly, the second direction is to develop the method for managing a multi-stack micro-grid with nonlinear models. The methodology proposed in Section 4.2.3 can be applied to other stochastic programmings, however, it is impossible to extend it to a non-linear problem since stochastic tube method currently is applicable to linear programming. To analyze correlations climatic variability to micro-grids based on nonlinear models, scenario-based method or scenario-tree based method is essential among stochastic programming approaches [60]. In this case, the number of variables increases rapidly with the number of the stacks, thus an algorithm should be ensure the efficient computations.

In addition, it is necessary to implement a design that reflects the factors caused by technological advancement since the performance of equipment used in the micro-grid is rapidly developing. For instance, the performances of batteries such as energy density, lifetime, and safety affect economic feasibility and structure of a micro-grid, thus these factors should be considered in the design problem of the micro-grid. Energy density, especially energy density per price, is related to the specifications of equipment, and it influences on the NPC of each equipment. Instead of using fixed spec-

ifications, the energy density advancement can be taken into account in the objective function by reflecting the change in specifications according to the annual energy density development. An increase in the lifetime of the equipment also causes a change in the replacement cycle, resulting in a change in NPC. As with energy density, this can be considered via an objective function that reflects the equipment's changing lifetime over the years. Battery's safety has an effect on the operational strategy, and it can be reflected in the constraints. For example, the battery's SoC has more marginal allowable range, or the constraints that prevent sudden fluctuations in the SoC becomes unnecessary. For other devices, Modifying the objective function or constraints in the same way, it is possible to design a microgrid considering technological development.

At last, economic size decision of multi-stack micro-grids should be conducted in more variety of regional climates rather than two regions to clarify climatic effects on a best operating level and narrow the search range of grid search. In addition, extending simulation time up to a year, techno-economic analysis integrated with EMS should be implemented to consider scheduling of a multi-stack micro-grid and climatic variability simultaneously.

Bibliography

[1] C. J. Rhodes, "The 2015 paris climate change conference: Cop21," *Science Progress*, vol. 99, no. 1, pp. 97–104, 2016.

[2] A. E. Dessler, *Introduction to modern climate change*. Cambridge University Press, 2021.

[3] Z. Fatima, M. Ahmed, M. Hussain, G. Abbas, S. Ul-Allah, S. Ahmad, N. Ahmed, M. A. Ali, G. Sarwar, P. Iqbal, *et al.*, "The fingerprints of climate warming on cereal crops phenology and adaptation options," *Scientific Reports*, vol. 10, no. 1, pp. 1–21, 2020.

[4] M. Papież, S. Śmiech, and K. Frodyma, "Effects of renewable energy sector development on electricity consumption–growth nexus in the european union," *Renewable and Sustainable Energy Reviews*, vol. 113, p. 109276, 2019.

[5] D. Li, C. Gao, T. Chen, X. Guo, and S. Han, "Planning strategies of power-to-gas based on cooperative game and symbiosis cooperation," *Applied Energy*, vol. 288, p. 116639, 2021.

[6] F. Egli, B. Steffen, and T. S. Schmidt, "A dynamic analysis of financing conditions for renewable energy technologies," *Nature Energy*, vol. 3, no. 12, pp. 1084–1092, 2018.

[7] M. F. Ishraque, S. A. Shezan, M. Ali, and M. Rashid, "Optimization of load dispatch strategies for an islanded microgrid connected with renewable energy sources," *Applied Energy*, vol. 292, p. 116879, 2021.

[8] K. Anoune, M. Ghazi, M. Bouya, A. Laknizi, M. Ghazouani, A. B. Abdellah, and A. Astito, "Optimization and techno-economic analysis of photovoltaic-wind-battery based hybrid system," *Journal of Energy Storage*, vol. 32, p. 101878, 2020.

[9] L. Kong, L. Li, G. Cai, C. Liu, P. Ma, Y. Bian, and T. Ma, "Techno-economic analysis of hydrogen energy for renewable energy power smoothing," *International Journal of Hydrogen Energy*, vol. 46, no. 3, pp. 2847–2861, 2021.

[10] D. Fares, M. Fathi, and S. Mekhilef, "Performance evaluation of metaheuristic techniques for optimal sizing of a stand-alone hybrid pv/wind/battery system," *Applied Energy*, vol. 305, p. 117823, 2022.

[11] M. H. Amrollahi and S. M. T. Bathaee, "Techno-economic optimization of hybrid photovoltaic/wind generation together with energy storage system in a stand-alone micro-grid subjected to demand response," *Applied Energy*, vol. 202, pp. 66–77, 2017.

[12] Z. Abdin and W. Mérida, "Hybrid energy systems for off-grid power supply and hydrogen production based on renewable energy: A techno-economic analysis," *Energy Conversion and Management*, vol. 196, pp. 1068–1079, 2019.

[13] H. Tebibel and A. Khellaf, "Techno-economic analysis of an off grid hybrid renewable energy system for hydrogen production," in *2017 International Renewable and Sustainable Energy Conference (IRSEC)*, pp. 1–6, IEEE, 2017.

[14] Y. Kalinci, A. Hepbasli, and I. Dincer, "Techno-economic analysis of a stand-alone hybrid renewable energy system with hydrogen production and storage options," *International Journal of Hydrogen Energy*, vol. 40, no. 24, pp. 7652–7664, 2015.

[15] G. Merei, C. Berger, and D. U. Sauer, "Optimization of an off-grid hybrid pv–wind–diesel system with different battery technologies using genetic algorithm," *Solar Energy*, vol. 97, pp. 460–473, 2013.

[16] B. Zhao, X. Zhang, P. Li, K. Wang, M. Xue, and C. Wang, "Optimal sizing, operating strategy and operational experience of a stand-alone microgrid on dongfushan island," *Applied Energy*, vol. 113, pp. 1656–1666, 2014.

[17] S. Vuddanti and S. R. Salkuti, "Review of energy management system approaches in microgrids," *Energies*, vol. 14, no. 17, p. 5459, 2021.

[18] J. Sarshar, S. S. Moosapour, and M. Joorabian, "Multi-objective energy management of a micro-grid considering uncertainty in wind power forecasting," *Energy*, vol. 139, pp. 680–693, 2017.

[19] E. C. Umeozor and M. Trifkovic, "Operational scheduling of microgrids via parametric programming," *Applied Energy*, vol. 180, pp. 672–681, 2016.

[20] A. Baziar and A. Kavousi-Fard, "Considering uncertainty in the optimal energy management of renewable micro-grids including storage devices," *Renewable Energy*, vol. 59, pp. 158–166, 2013.

[21] D. H. Vu, K. M. Muttaqi, D. Sutanto, *et al.*, "An integrated energy management approach for the economic operation of industrial microgrids under uncertainty of renewable energy," *IEEE Transactions on Industry Applications*, vol. 56, no. 2, pp. 1062–1073, 2020.

[22] N. Herr, J.-M. Nicod, C. Varnier, L. Jardin, A. Sorrentino, D. Hissel, and M.-C. Péra, "Decision process to manage useful life of multi-stacks fuel cell systems under service constraint," *Renewable Energy*, vol. 105, pp. 590–600, 2017.

[23] J. Zhao, S. Cai, X. Luo, and Z. Tu, "Multi-stack coupled energy management strategy of a pemfc based-cchp system applied to data centers," *International Journal of Hydrogen Energy*, vol. 47, no. 37, pp. 16597–16609, 2022.

[24] A. J. Calderón, F. J. Vivas, F. Segura, and J. M. Andújar, "Integration of a multi-stack fuel cell system in microgrids: A solution based on model predictive control," *Energies*, vol. 13, no. 18, p. 4924, 2020.

[25] H. Babazadeh, B. Asghari, and R. Sharma, "A new control scheme in a multi-battery management system for expanding microgrids," in *ISGT 2014*, pp. 1–5, IEEE, 2014.

[26] F. T. Moore, "Economies of scale: Some statistical evidence," *The Quarterly Journal of Economics*, vol. 73, no. 2, pp. 232–245, 1959.

[27] C. Gu, C. Tang, Y. Xiang, and D. Xie, "Power-to-gas management using robust optimisation in integrated energy systems," *Applied Energy*, vol. 236, pp. 681–689, 2019.

[28] Y. Zhang, F. Meng, R. Wang, W. Zhu, and X.-J. Zeng, "A stochastic mpc based approach to integrated energy management in microgrids," *Sustainable Cities and Society*, vol. 41, pp. 349–362, 2018.

[29] I. Gomes, R. Melicio, and V. Mendes, "A novel microgrid support management system based on stochastic mixed-integer linear programming," *Energy*, vol. 223, p. 120030, 2021.

[30] X. Guo, Z. Bao, Z. Li, and W. Yan, "Adaptively constrained stochastic model predictive control for the optimal dispatch of microgrid," *Energies*, vol. 11, no. 1, p. 243, 2018.

[31] A. Baziar and A. Kavousi-Fard, "Considering uncertainty in the optimal energy management of renewable micro-grids including storage devices," *Renewable Energy*, vol. 59, pp. 158–166, 2013.

[32] F. Conte, G. Mosaico, G. Natrella, M. Saviozzi, and F. R. Bianchi, "Optimal management of renewable generation and uncertain demand with reverse fuel cells by stochastic model predictive control," in *2022 17th International Conference on Probabilistic Methods Applied to Power Systems (PMAPS)*, pp. 1–6, IEEE, 2022.

[33] E. C. Umeozor and M. Trifkovic, "Operational scheduling of microgrids via parametric programming," *Applied Energy*, vol. 180, pp. 672–681, 2016.

[34] A. Perera, V. M. Nik, D. Chen, J.-L. Scartezzini, and T. Hong, "Quantifying the impacts of climate change and extreme climate events on energy systems," *Nature Energy*, vol. 5, no. 2, pp. 150–159, 2020.

[35] A. Diaz-Papkovich, L. Anderson-Trocmé, and S. Gravel, "A review of umap in population genetics," *Journal of Human Genetics*, vol. 66, no. 1, pp. 85–91, 2021.

[36] D. Kobak and G. C. Linderman, "Initialization is critical for preserving global data structure in both t-sne and umap," *Nature Biotechnology*, vol. 39, no. 2, pp. 156–157, 2021.

[37] E. Becht, L. McInnes, J. Healy, C.-A. Dutertre, I. W. Kwok, L. G. Ng, F. Ginhoux, and E. W. Newell, "Dimensionality reduction for visualizing single-cell data using umap," *Nature Biotechnology*, vol. 37, no. 1, pp. 38–44, 2019.

[38] L. McInnes, J. Healy, and J. Melville, "Umap: Uniform manifold approximation and projection for dimension reduction," *arXiv preprint arXiv:1802.03426*, 2018.

[39] J. Liu, S. Sun, and C. Chen, "Big data analysis of regional meteorological observation based: on hierarchical density clustering algorithm hdbscan," in *2021 2nd International Seminar on Artificial Intelligence, Networking and Information Technology (AINIT)*, pp. 111–116, IEEE, 2021.

[40] F. Terroso-Saenz and A. Munoz, "Land use discovery based on volunteer geographic information classification," *Expert Systems with Applications*, vol. 140, p. 112892, 2020.

[41] A. Baqir, S. ul Rehman, S. Malik, F. ul Mustafa, and U. Ahmad, "Evaluating the performance of hierarchical clustering algorithms to detect spatio-temporal crime hot-spots," in *2020 3rd International Conference on Computing, Mathematics and Engineering Technologies (iCoMET)*, pp. 1–5, IEEE, 2020.

[42] C. Ghenai and M. Bettayeb, "Modelling and performance analysis of a stand-alone hybrid solar pv/fuel cell/diesel generator power system for university building," *Energy*, vol. 171, pp. 180–189, 2019.

[43] T. Lambert, P. Gilman, and P. Lilienthal, "Micropower system modeling with homer," *Integration of Alternative Sources of Energy*, vol. 1, no. 1, pp. 379–385, 2006.

[44] J. M. Lujano-Rojas, R. Dufo-López, and J. L. Bernal-Agustín, "Optimal sizing of small wind/battery systems considering the dc bus voltage stability effect on energy capture, wind speed variability, and load uncertainty," *Applied Energy*, vol. 93, pp. 404–412, 2012.

[45] R. Dufo-López, "Optimisation of size and control of grid-connected storage under real time electricity pricing conditions," *Applied Energy*, vol. 140, pp. 395–408, 2015.

[46] C. Ghenai and M. Bettayeb, "Modelling and performance analysis of a stand-alone hybrid solar pv/fuel cell/diesel generator power system for university building," *Energy*, vol. 171, pp. 180–189, 2019.

[47] N. Aeronautics and S. A. L. R. Center., "Power data access viewer v2.0.0.," 2022. datashare `https://power.larc.nasa.gov/data-access-viewer/`.

[48] R. J. Campello, D. Moulavi, and J. Sander, "Density-based clustering based on hierarchical density estimates," in *Pacific-Asia conference on knowledge discovery and data mining*, pp. 160–172, Springer, 2013.

[49] R. J. Campello, D. Moulavi, A. Zimek, and J. Sander, "Hierarchical density estimates for data clustering, visualization, and outlier detection," *ACM Transactions on Knowledge Discovery from Data (TKDD)*, vol. 10, no. 1, pp. 1–51, 2015.

[50] F. Amjad and L. A. Shah, "Identification and assessment of sites for solar farms development using gis and density based clustering technique-a case of pakistan," *Renewable Energy*, vol. 155, pp. 761–769, 2020.

[51] Y. Zhao, L. Ye, W. Wang, H. Sun, Y. Ju, and Y. Tang, "Data-driven correction approach to refine power curve of wind farm under wind

curtailment," *IEEE Transactions on Sustainable Energy*, vol. 9, no. 1, pp. 95–105, 2017.

[52] R. Dey and S. Chakraborty, "Convex-hull & dbscan clustering to predict future weather," in *2015 International Conference and Workshop on Computing and Communication (IEMCON)*, pp. 1–8, IEEE, 2015.

[53] J. Zhang and Y. Zhang, "Forecast of photovoltaic power generation based on dbscan," in *E3S Web of Conferences*, vol. 236, p. 02016, EDP Sciences, 2021.

[54] D. Moulavi, P. A. Jaskowiak, R. J. Campello, A. Zimek, and J. Sander, "Density-based clustering validation," in *Proceedings of the 2014 SIAM International Conference on Data Mining*, pp. 839–847, SIAM, 2014.

[55] H. Tebibel and A. Khellaf, "Techno-economic analysis of an off grid hybrid renewable energy system for hydrogen production," *2017 International Renewable and Sustainable Energy Conference (IRSEC)*, pp. 1–6, 2017.

[56] C. Ghenai and M. Bettayeb, "Modelling and performance analysis of a stand-alone hybrid solar pv/fuel cell/diesel generator power system for university building," *Energy*, vol. 171, pp. 180–189, 2019.

[57] Z. Liu, J. Guo, D. Wu, G. Fan, S. Zhang, X. Yang, and H. Ge, "Two-phase collaborative optimization and operation strategy for a new distributed energy system that combines multi-energy storage for a nearly zero energy community," *Energy Conversion and Management*, vol. 230, p. 113800, 2021.

[58] P. J. Rousseeuw, "Silhouettes: a graphical aid to the interpretation and validation of cluster analysis," *Journal of Computational and Applied Mathematics*, vol. 20, pp. 53–65, 1987.

[59] J. Yu, J.-H. Ryu, and I.-b. Lee, "A stochastic optimization approach

to the design and operation planning of a hybrid renewable energy system," *Applied Energy*, vol. 247, pp. 212–220, 2019.

[60] A. Mesbah, "Stochastic model predictive control: An overview and perspectives for future research," *IEEE Control Systems Magazine*, vol. 36, no. 6, pp. 30–44, 2016.

[61] M. Shi, H. Wang, C. Lyu, P. Xie, Z. Xu, and Y. Jia, "A hybrid model of energy scheduling for integrated multi-energy microgrid with hydrogen and heat storage system," *Energy Reports*, vol. 7, pp. 357–368, 2021.

초 록

전세계적인 기후 위기의 증가를 대처하기 위해서 재생가능한 에너지원을 기반으로 하는 마이크로 그리드 (micro-grid) 는 중심 기술이 되고 있다. 재생 에너지는 마이크로 그리드에 필수적이지만 간헐적인 특성과 강한 불확실성을 가지고 있어 기후 변동성이 마이크로 그리드의 핵심 문제이다. 그럼에도 불구하고, 기존의 마이크로 그리드의 기술 경제성 분석들은 기후 변동성을 거의 고려하지 않았으며, 다중 스택 (multi-stack) 마이크로 그리드의 에너지 크기 조정 및 에너지 관리와 관련된 연구는 거의 없다. 우리는 이러한 문제를 해결하기 위해 빅 데이터 기반 분석과 혼합 정수 확률론적 기반의 (mixed-integer stochastic) 에너지 관리를 활용하였다. 218개국 13,488개 지역의 기후 데이터를 활용하여 기술 경제 분석의 기후 변동성을 조사하였다. 균일한 매니폴드 근사 및 투영 (uniform manifold approximation and projection) 을 통해 데이터를 전처리한 후 노이즈를 사용한 계층적 밀도 기반 공간 클러스터링 (hierarchical density-based spatial clustering of applications with noise) 알고리즘을 사용하여 차원 축소된 데이터를 클러스터링하고, 기후 패턴에 따라서 클러스터의 마이크로 그리드의 최적 크기를 서로 비교하였다. 기후 민감도 분석으로 마이크로 그리드의 규모와 비용에 기후가 미치는 영향을 밝혀냈으며, 이는 마이크로 그리드의 설계 시 기후 변동을 고려할 필요성을 강조한다. 다중 스택 마이크로 그리드의 구조와 스택의 크기를 결정하기 위해서 우리는 기후 불확정성의 존재하에서 다중 스택 마이크로 그리드의 에너지 관리에 적합한 혼합 정수 확률 프로그래밍 (mixed-integer stochastic programming) 를 제안하였다. 각각의 예시 문제를 통해서 제안된 방법이 유효한 것을 확인한

이후에 다중 스택 마이크로 그리드의 설계에 기후가 영향을 미치는 것을 입증하였다. 결과적으로, 이는 재생 에너지 기반의 마이크로 그리드에서 기후 변동성이 중요한 역할을 하는 것을 시사한다. 본 학위논문이 제시하는 분석 및 방법의 특징은 다음과 같이 요약할 수 있다. 우선, 기후 변동성이 기술 경제적인 마이크로 그리드의 설계의 결정 요인 중 하나라는 것을 확인하기 위해서 비지도학습 클러스터링 (unsupervised clustering) 을 이용한 관계성 분석을 시행하였다. 균일한 매니폴드 근사 및 투영과 노이즈를 사용한 계층적 밀도 기반 공간 클러스터링 알고리즘을 사용하여 218개국가의 13,844개 지역의 기후 데이터의 노이즈를 완화시키고 클러스터링을 진행하였다. 다음으로, 지역적인 기후 특징을 바탕으로 마이크로 그리드의 설치와 장기적인 운영을 위한 전략을 제안하였다. 세번째로는, 다중 스택 마이크로 그리드의 에너지 분배를 제어하기 위해서 혼합 정수 확률 프로그래밍 방법론을 개발하였다. 마지막으로, 다중 스택 마이크로 그리드 설계에서 기후 영향이 두드러짐을 확인했다.

주요어 : 마이크로 그리드, 재생가능한 에너지, 빅데이터 분석, 기술경제성 분석, 민감도 분석, 에너지 관리 시스템, 혼합 정수 확률 프로그래밍, 규모의 경제

학번 : 2017-22082